Concrete Materials and Structural Integrity Research Group

Department of Civil Engineering
University of Cape Town, South Africa
Private Bag X3, Rondebosch 7701

Tel.: +27 (0) 21 6502603
Fax: +27 (0)21 6897471
Website: http://www.csirg.uct.ac.za

Research report

Transport mechanisms in concrete

Corrosion of steel in concrete

(Initiation, propagation & factors affecting)

Assessment of corrosion

Compiled by Mr Mike Otieno, Prof. Mark Alexander and Dr Hans Beushausen

TABLE OF CONTENTS

List of Figures

List of Tables

Chapter 1

: TRANSPORT MECHANISMS IN CONCRETE

1 TRANSPORT MECHANISMS IN CONCRETE

1.1 ***Introduction***

Transport properties of cementitious materials are a key factor for predicting their durability, since deterioration mechanisms such as corrosion, leaching or carbonation are all related to the ease with which a fluid or ion can move through the concrete microstructure. The passage of potentially aggressive species is primarily influenced by the penetrability of the concrete. Penetrability is broadly defined as the degree to which a material permits the transport through it of gases, liquids, or ionic species. It embraces the concepts of permeability, sorption, diffusion and migration/conduction and is quantifiable in terms of the transport parameters (Alexander and Mindess, 2005). For a durable RC structure, limiting the movement of fluids is one of the functions it has to fulfil (Breysse and Gerard, 1997, Stanish *et al*., 2004).

The processes involved in fluid and ion movement include the distinct mechanisms of capillary action, fluid flow under pressure, flow under a concentration gradient, and movement due to an applied electric field. These mechanisms are characterised by the material properties of sorptivity, permeability, diffusivity and conduction/migration respectively (Richardson, 2002). The permeability of concrete will predominantly be influenced by the permeability of the cement paste, especially at the interface with aggregate particles.

The transport mechanisms will be dealt with firstly for uncracked concrete but cracked concrete will also be covered in section 1.9 will deal with cracked

Concrete transport parameters relate to the mechanisms of diffusion, migration/conduction, permeation, sorption, convection and wick action. These are covered in the following sections.

1.2 ***Diffusion***

Diffusion is the movement of gases, ions and/or molecules under the influence of a concentration gradient, from an area of high concentration to one with a low concentration. Gaseous diffusion is experienced in unsaturated concrete while ionic diffusion occurs in saturated and partially saturated conditions. Molecular diffusion takes place if the pores of the medium are relatively large (Sharif *et al.*, 1999).

The modelling of gaseous and ionic diffusion in concrete is commonly done using Fick's first law of diffusion (for steady state diffusion). This law may be used to describe the rate of diffusion of a gas/ion through a uniformly diffusable material (Richardson, 2002):

$$J = -D_{eff}\frac{dC}{dx} \tag{1.1}$$

where J = mass transport rate (g/m^2s)
D_{eff} = effective diffusion coefficient (m^2/s)
dC/dx = concentration gradient ($g/m^3/m$)
C = Concentration of fluid (ion or gas)
x = distance (m)

The negative prefix denotes that the flux occurs along a negative concentration gradient.

The modelling of ionic diffusion in concrete is done using Fick's second law of diffusion (for non-steady state diffusion) as will be seen in section 2.3.5.2. The penetration of chloride ions through concrete is best represented by diffusion process if the concrete is assumed to be relatively saturated (Kim and Stewart, 2000).

Diffusion acts as a predominant mechanism for concrete structures fully submerged in sea water or salt-contaminated soil. In combination with other mechanisms, diffusion contributes to chloride transport in concrete under most exposure conditions. The transport of oxygen in concrete to the steel surface is also governed mainly by diffusion process. The rate of diffusion of oxygen is determined by the pore structure, pore size distribution of concrete and its moisture content. It decreases sharply with the increase in moisture content (Richardson, 2002).

1.3 ***Migration***

Migration (also referred to as *accelerated diffusion*, *electro-diffusion*, or *conduction*) is the movement of ions in a solution under an electrical field. It is main the transport mechanism in laboratory-accelerated chloride tests, and is governed by the Nernst-Planck equation (Andrade, 1993):

$$v = \left(D\frac{zF}{RT}\right)\left(\frac{dU}{dx}\right) \tag{1.2}$$

where v = velocity of the ionic species
D = diffusion coefficient of the ionic species
z = electrical charge (ionic valence) of diffusing ions

F = Faraday's constant (9.6548 x 10^4 J/Vmol)

T = absolute temperature

U = potential difference across the sample

x = distance variable

R = universal gas constant (8.314 J/molK)

In many tests, diffusion and migration may occur mostly at the same time and the total flux is the sum of both (Stanish *et al*., 2004). However in most cases, migration accounts for the greatest part of the flux.

1.4 ***Permeation***

Permeability of concrete is defined as a measure of the capacity of concrete to transfer fluids through its pore structure under an externally applied pressure whilst the pores are saturated with that fluid. The driving force for liquids and gases through the pore spaces or crack networks is a pressure gradient (Samaha and Hover, 1992).

For permeation, D'Arcy's law is used to calculate average velocity of flow of the fluid ($\bar{v}$):

$$\bar{v} = \left(\frac{k}{n}\right)\left(-\frac{dh}{dx}\right) \qquad \text{check Kropp and Alexander} \tag{1.3}$$

where k = permeability coefficient

n = porosity

h = hydraulic head

x = distance

Permeation plays an important role in water retaining structures where water transport through the structure is detrimental.

1.5 ***Sorption***

Sorption refers to uptake of liquids into an unsaturated or partially saturated solid by capillary suction. It is measured using parameters such as bulk absorption, or sorptivity S. Sorptivity is essentially the movement of a wetting front in a dry or partially saturated porous medium (Alexander and Mindess, 2005):

$$\mathrm{S} = \frac{\Delta M_t}{t^{1/2}}\left[\frac{d}{M_{sat} - M_o}\right] \tag{1.4}$$

where $\Delta M/t^{1/2}$ = slope of the straight line produced when the mass of water absorbed is plotted against the square root of time

d = sample thickness

M_{sat} & M_o = saturated mass and dry mass of concrete specimen respectively

Sorptivity is influenced by the larger capillaries and their degree of continuity, and is very sensitive to hydration of the outer concrete surface, and hence curing. It is also influenced by compaction and aggregate orientation and distribution and by mix composition (Kropp and Hilsdorf, 1995).

1.6 ***Convection***

Convection (or *advection*) is the process that describes the transport of a solute (e.g. chloride or sulphate ions) as a result of the bulk moving water (Boddy *et al*., 1999). The process is described by:

$$\frac{\partial C}{\partial t} = -\bar{v}\,\frac{\partial^2 C}{\partial x^2} \tag{1.5}$$

where C = Concentration of solute at depth x after time t

$\bar{v}$ = average velocity vector of fluid flow

Convection (together with diffusion) is the main transport mechanism for chloride ingress in cracked concrete (Paulsson, and Johan, 2002). It also has an important role in the movement of chloride ions when concrete is exposed to drying-wetting conditions.

1.7 ***Wick action***

Wick action is the transport of water and the ions it may contain through a concrete structure from a face in contact with water/salt solution to a drying face (Figure 1.1). It may also occur in concrete exposed to wetting and drying cycles. Wick action is often dominated by convection (Buenfeld *et al.*, 1997). Chlorides can penetrate concrete by wick action. It results in a build-up of chlorides inside the concrete particularly near the drying face.

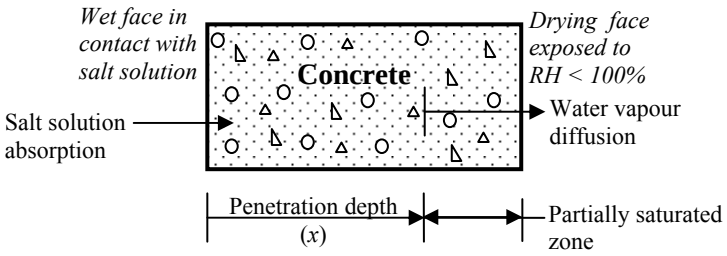

Figure 1.1: A schematic illustration of wick action in concrete (Puyate.and Lawrence, 1999)

1.8 ***Combined transport processes***

The selection in isolation of a single transport mechanism for the ingress of a particular substance may represent an over-simplification of the real transport process since more than one transport mechanism may be active at a given time, either in parallel or in different sections along the flow paths (Boddy *et al*., 1999, Kropp and Alexander, 2007).

To date, quantification of the combined transport processes (also referred to as *mixed modes of transport*) has not been fully achieved. To do this, an in-depth understanding of the individual mechanisms is mandatory. Studies on transport processes should aspire to obtain models for predicting simultaneous movement of the species (chlorides, sulphates, oxygen, carbon dioxide, moisture) including the deposition and dissolution of ions (Nilssson *et al*., 1996). In line with this, development should be made in the field of testing in order to develop testing methods that can assess combined transport mechanisms.

Considering chloride penetration into concrete alone, the combined transport processes are usually physically quantified in terms of chloride profiles showing the distribution of chlorides with depth from the concrete surface at different times of exposure.

1.9 ***Transport properties of cracked concrete***

Knowledge of the transport properties of cracked concrete is essential for predicting its durability since the deteriorating mechanisms (freeze and thaw, corrosion, leaching) depend on the flow of aggressive agents through the cracked concrete. The presence of cracks can significantly modify transport properties of concrete. Microcracks that are discrete and well distributed will influence transport in a very different manner compared to visible, connected, localised macrocracks. Transport in a cracked concrete is therefore a coupled phenomenon between the matrix and the crack (Mohamed *et al*., 2003).

However, since the kinetics of different transport processes varies, changes resulting from cracking greatly depend on the mechanism which is predominant. For instance, an increase in

permeability as a direct result of cracking can be of several orders of magnitude, while diffusivity is much less affected by cracks (Rodriguez, 2001, Weiss *et al*., 2007)

Moreover, it has been shown that the main parameters for describing flow in damaged and sound material are different; for example in uncracked concrete permeability is related to its porosity, while in cracked concrete it is related to crack properties. Regardless of the transport mechanism, properties of cracks become more important in cracked concrete than the properties of concrete itself. Parameters, such as crack width and shape, crack density/frequency and degree of connectivity, as well as crack origin, govern transport in cracked concrete (Breysse and Gerard, 1997). Therefore, no predictions on the behaviour of cracked concrete may be made based on the data for uncracked concrete.

Transport processes in cracked concrete can be studied using methods such as numerical simulation/modelling (Frederiksen *et al.*, 1997, Breysse and Gerard, 1997, Gerard and Marchand, 2000, Marsavina *et al*., 2007), feedback-controlled splitting tests (Aldea *et al*., 1999) and imitation of various cracking mechanisms that concrete structures encounter under actual service conditions, as well as the creation of artificial cracks e.g. by positioning of shims in the mould prior to casting.

Therefore, either model (simulated) or artificial cracks could be used in studying cracked concrete, as they are much easier to characterize and control than actual cracks. However, any models derived from experimenting with artificial cracks should always be calibrated on real concrete structures to ensure their reliability.

1.10 Effect of concrete aging on transport mechanisms

Within its service life, the transport properties of concrete are most likely to be modified. This is mainly due to the ongoing hydration of the cementitious material but can also result from deterioration of the material. As a result, the porosity as well as the continuity of the capillary porosity may decrease with time. Other processes such as chloride binding also continue during this time (Gerard and Marchand, 2000). This is of considerable importance when transport parameters are assessed in laboratory experiments on young concrete specimens to provide input data for long term assessment of structures, e.g. service life prediction.

Therefore, the transport characteristics of concrete also change with time and should be considered. One way of taking into consideration the effect of concrete aging is by using time functions (Mackechnie, 1996, Basheer *et al*., 2001, Kropp and Alexander, 2007). An example is given in chapter 2 section 2.3.5.2.

Chapter 2

: CORROSION OF STEEL IN CONCRETE

2 CORROSION OF STEEL IN CONCRETE

2.1 Introduction

Reinforcement corrosion is one of the main durability-threatening mechanisms in reinforced concrete (RC). Much research has focused on increasing the basic understanding of both the transport mechanisms of aggressive ions (chloride ions) through concrete and the subsequent corrosion of reinforcing steel (Tuutti, 1982, Mackechnie, 1996, Schiessl, 1998, Glass and Buenfeld, 1997).

The degradation of RC structures mainly involves three stages as shown in Figure 2.1, (Heckroodt, 2002):

(i) An initiation period before corrosion activation, during which little deterioration occurs.

(ii) A propagation period after corrosion activation that generates expansive corrosion products causing cracking of the cover concrete.

(iii) An acceleration period where corrosion rate increases due to easy access of oxygen, water and further aggressive agents through cracks and spalls.

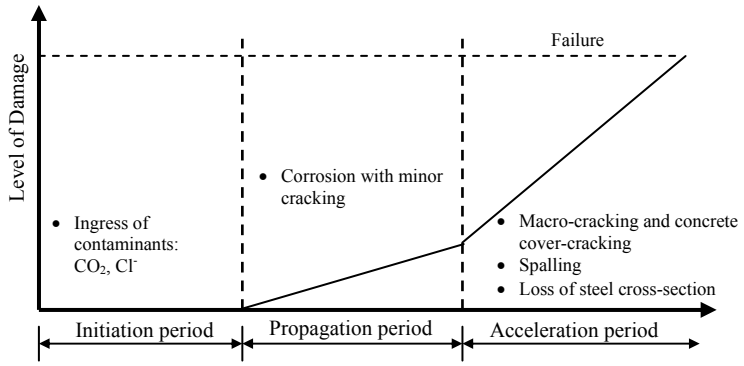

Figure 2.1: Three-stage corrosion damage model (Heckroodt, 2002)

The acceleration period depicts a time when visible corrosion damage is clearly evident and the penetrability of concrete cover may be of little value in controlling corrosion rate due to extensive macro-cracking and spalling. The boundary between the propagation and acceleration stages may be dependent on factors such as tensile strength of the concrete.

2.2 Fundamentals of steel corrosion in concrete

Corrosion may be defined as the surface wastage that occurs when metals are exposed to reactive environments. It is an electrochemical process in which iron enters into solution at the anode and an oxidizing agent is reduced at the cathode. It results in the flow of electrons

between anodic and cathodic sites on the steel. The fundamental cause of corrosion is the inherent instability of metals in the metallic form. The tendency is for metals to revert to more stable forms, such as their oxides, hydroxides or sulphides (Heckroodt, 2002).

The conventional steel grades commonly used as reinforcing steel in concrete are susceptible to corrosion when exposed to the atmosphere. However, steel embedded in concrete is naturally protected by the high alkalinity of the cement matrix (pH > 12.5) and by the barrier effect of the concrete cover. The concrete cover limits the amount of oxygen, moisture, carbon dioxide and chlorides which are required for active corrosion. The high alkalinity results from the presence of sodium hydroxide (*NaOH*) and potassium hydroxide (*KOH*), due to the dominant alkalis in the cement i.e. sodium oxide (Na_2O) and potassium oxide (K_2O), in a saturated calcium hydroxide solution ($Ca(OH)_2$). Without ingress of corrosive species such as carbon dioxide and chlorides into concrete during its service life, reinforcing steel passivates due to the alkaline concrete pore solution, resulting in negligible corrosion rates. The high pH suppresses steel corrosion by encouraging the formation of a very thin (1-10 nm thick) passive ferric oxide film (maghemite, $\gamma - Fe_2O_3$) on the steel surface (Richardson, Heckroodt, 2002).

For corrosion to occur four basic elements are required:

(i) Anode – site where corrosion occurs and from which current flows.

(ii) Cathode – site where corrosion does not occur but to which corrosion current flows.

(iii) Electrolyte – a medium capable of conducting electric current by ionic current flow. In case of concrete, the electrolyte is constituted by the pore solution, which is alkaline.

(iv) Metallic path – connection between the anode and cathode, which allows current return and completes the circuit. Steel serves this purpose in reinforced concrete (Figure 2.2).

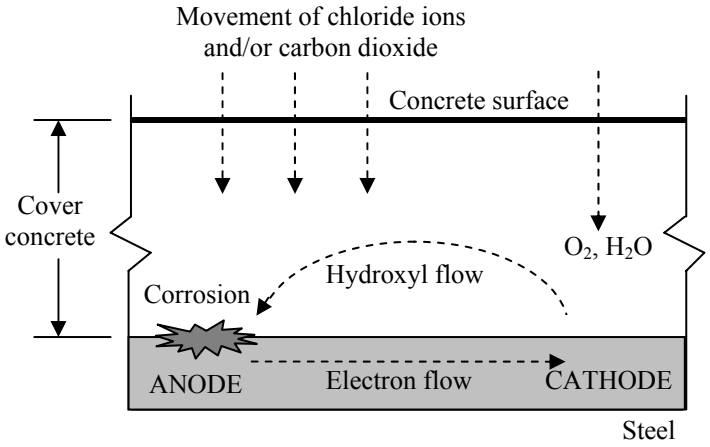

Figure 2.2: A schematic illustration of the corrosion process in concrete (Mackechnie *et al*., 2001)

The basic anodic reaction for steel embedded in concrete is (Bockris *et al*., 1981):

$$Fe \rightarrow Fe^{2+} + 2e^{-} \quad (2.1)$$

Electrons released at the anode are consumed at the cathode by reduction. The possible cathodic reactions depend on the availability of O_2 and on the pH in the vicinity of the steel surface. The most likely reaction is (Bockris *et al*., 1981):

$$2H_2O + O_2 + 4e^{-} \rightarrow 4OH^{-} \quad (2.2)$$

There can be either microcell or macrocell corrosion of steel in concrete. Macrocell corrosion is characterised by a small anode and a large cathode i.e. the anode and cathode are clearly separated in different areas. It frequently occurs in chloride-induced corrosion and/or in concrete with a low resistivity (high conductivity). It is characterised by high local corrosion (pit corrosion) and steel cross-section reduction. In microcell corrosion the anodic and cathodic sites are adjacent to each other. It is more common in carbonation-induced corrosion and/or in concrete with high resistivity e.g. carbonated concrete (Bockris *et al*., 1981).

Although the passive film provides an effective protective layer, it is thin enough to permit electron transfer and hence sustain the cathodic reaction (West, 1980). The general properties of this passive layer include the following (Schreir, 1979):

(i) Very low ionic conductivity
(ii) Very low dissolution rate and chemical solubility
(iii) Appreciable electron conductivity
(iv) Good adhesion to the rebar
(v) A large range of potential thermodynamic stability

The passive layer can be disrupted by either reduction in alkalinity (e.g. carbonation) or by chloride attack. After depassivation corrosion may occur and propagate depending on the availability of corrosion agents (chlorides, carbon dioxide, moisture and oxygen).

2.2.1 ***Corrosion of steel in cracked concrete***

In cracked concrete, corrosion starts either in the crack zone or in the areas immediately adjacent to the crack. There are two different corrosion mechanisms that are theoretically possible in the region of cracks (Schiessl and Raupach, 1997):

Mechanism I: Where both the anodic and cathodic sites are in the zone of the crack. Anodic and cathodic areas are very small and located close to each other (microcell

corrosion). The oxygen required for the cathodic reaction is supplied through the crack.

Mechanism II: Where the reinforcement in the crack zone acts as an anode, and the passive steel surface between the cracks forms the cathode. In this instance, oxygen penetrates mainly through the uncracked area of the concrete (macrocell corrosion). The steel surface involved in this corrosion process is larger than in the first mechanism, hence, higher corrosion currents can be expected.

2.2.2 ***Corrosion products***

The primary reaction for the corrosion of iron is the conversion of Fe to Fe^{2+} in the aqueous solution. Numerous hydroxides, oxides and oxide-hydroxides of iron form under different conditions of temperature, pressure, potential and pH (Cornell and Schwertmann, 1996).

The variations in volume change associated with individual iron oxides are clearly illustrated in Figure 2.3.

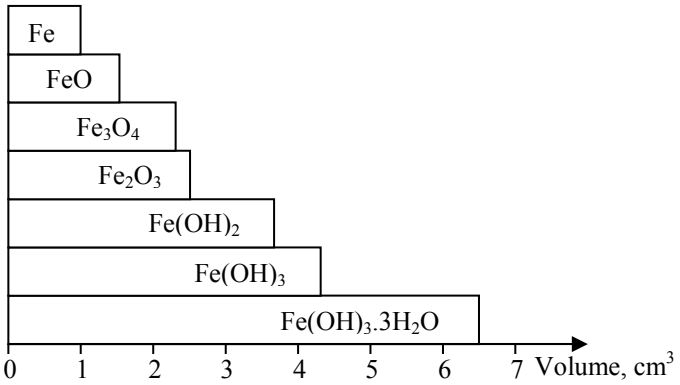

Figure 2.3: Relative volume of iron corrosion products (Liu, 1996)

2.3 ***Corrosion initiation***

Corrosion of steel in RC can be caused by several factors including ingress of chlorides, carbon dioxide, stray currents and bacterial attack. However, the main causes that will be discussed in this section are carbonation-induced and chloride-induced corrosion. Corrosion initiation is defined as the point at which the steel (or a part of it) becomes depassivated and starts to corrode actively, even if at low corrosion rate initially. Focus is placed on chloride-induced corrosion.

2.3.1 ***Initiation of carbonation-induced corrosion***

Carbonation is a neutralising reaction in the cement paste that reduces the pH from above 12 to less than 9 (Parrott, 1995). It occurs in concrete when carbon dioxide (CO_2) reacts with water, calcium, alkaline hydroxides and cement phases to form calcium carbonate ($CaCO_3$)

and of silica and alumina gel, resulting in the lowering of the pore solution pH to values between 8.5 and 9.0.

The carbonation process involves the following stages. First, the atmospheric carbon dioxide reacts with water in the concrete pores to form carbonic acid.

$$H_2O + CO_2 \rightarrow H_2CO_3 \tag{2.3}$$

This is followed by reaction of the carbonic acid with $Ca(OH)_2$ in the concrete as follows:

$$H_2CO_3 + Ca(OH)_2 \rightarrow CaCO_3 + 2H_2O \tag{2.4}$$

The above process leads to the depassivation of the steel in contact with the carbonated zones. The water released during the chemical reactions can sustain both the formation of carbonic acid and the carbonation process. Hence when carbonation starts, it is almost self-sustaining because of this release of water; but it can be limited due to the increasing difficulty for the carbon dioxide to penetrate into the depth of the concrete (Richardson, 2002). Under conditions of strong carbonation or after long periods, the calcium silicate hydrates can become carbonated, resulting in the formation of silica and alumina gel.

The carbonates formed in the carbonation reaction are larger molecules than the hydroxides, thereby increasing the density of the cement paste and locally, the strength (Neville, 1996). The formation of carbonic acid lowers the pH of the concrete pore solution. As soon as the carbonation front reaches the steel, in the presence of water and oxygen, the corrosion process begins.

Carbonation is a diffusion process and therefore its depth (i.e. carbonation front) progresses by an exponential decrease with time. The modelling of carbonation is generally made by means of the simplified expression (Richardson, 2002):

$$x = K_{co_2} \sqrt{t} \tag{2.5}$$

where x = carbonation depth after time t

K_{co_2} = carbonation factor of the particular concrete

It does not develop if the concrete is water-saturated or in very dry conditions. This is because (a) moisture is required to form carbonic acid which attacks the $Ca(OH)_2$ and (b) CO_2 is not readily soluble in water.

Carbonation usually induces a generalized (macrocell) type of corrosion i.e. there are neither distinct anodes nor cathodes. Optimal conditions for increased carbonation rates include temperatures near 20 °C, relative humidity in the range of 50-70%, increased carbon dioxide concentration, w/b ratios at or above 0.6, and use of fly ash or slag as a cement replacement. At equal w/b ratios, pozzolanic concretes (e.g. concretes incorporating fly ash or slag) are less capable of resisting carbonation than Portland cement concretes owing to their lower $Ca(OH)_2$ (portlandite) content (Sisomphon *et al*., 2007). Concrete intrinsic factors tend to have the greatest impact on carbonation rates. The most important is the w/b ratio. Carbonation is often greatly reduced at w/b ratios below approximately 0.4. A reduction in carbonation depth of approximately 50% is observed when the w/b ratio is reduced from 0.6 to 0.4 (Parrott, 1987).

There is no standard method to measure carbonation but several publications discuss different methods e.g. ASTM C 856 and Rilem Recommendation CPC 18. The most common method is spraying freshly broken concrete surfaces with 1% or 2% phenolphthalein solution. The surface where the pH is greater than 9 turns purple with gradually lightening shades of pink for pH of 8-9. The location where the surface is colourless represents the depth to which full or nearly full carbonation has been achieved and the pH of the cement is at or below approximately 8.

The phenolphthalein method is quick and economical, though it does not identify areas of partial carbonation. Rainbow indicators, which produce a range of colours for small changes of pH can be used in a similar method (Jana and Erlin, 2007). However, rainbow indicators require more subjective analysis in determining the location of the colour changes and the colours are not as vivid as the phenolphthalein indicator solution. Phenolphthalein indicator is therefore still widely used.

2.3.2 Initiation of chloride-induced corrosion

When chloride ions are introduced in concrete during mixing or after exposure to the environment, they may depassivate the steel by locally breaking down the protective layer, γ-Fe_2O_3. Chlorides act as a catalyst to corrosion when they are in sufficient concentration at the steel surface. They are not consumed in the process but help to break down the passive layer and allow corrosion to proceed faster (Figure 2.4) (Broomfield, 1997).

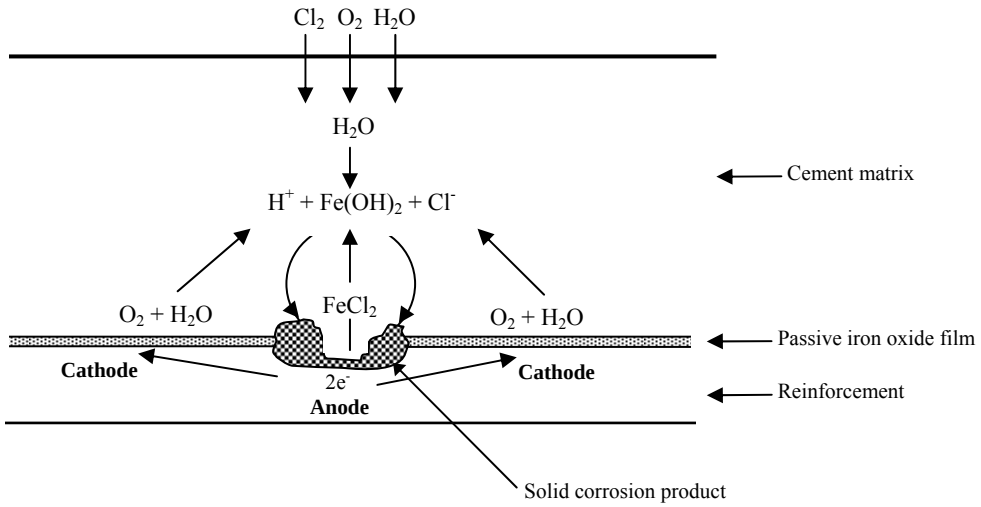

Figure 2.4: Corrosion of reinforcement in concrete exposed to chloride ions (Broomfield, 1997)

Chloride ions surrounding the reinforcement react at anodic sites to form hydrochloric acid, which destroys the passive protective film on the steel. The surface of the steel then becomes activated locally to form the anode, with the passive surface forming the cathode: the resulting corrosion is in the form of localised pitting (pit-corrosion). The chloride ions react with Fe^{2+} to form chloride or oxychloride compounds ($FeCl_2$ and FeOCl) (Melchers and Li, 2006):

The following cathodic reactions have been suggested to take place by Stanbury and Buchaman (2000):

$$Fe^{2+} + 2Cl^- \rightarrow FeCl_2 \qquad (2.6)$$

$$FeCl_2 + 2H_2O \rightarrow Fe(OH)_2 + 2\,HCl \qquad (2.7)$$

The process then becomes self-propagating, due to the acidic conditions created, and the recycling of chloride ions. This occurs through hydrolysis of the chloride compounds, such as given in equation (2.8):

$$FeOCl + H_2O \rightarrow Fe(OH)_2 + Cl^- \qquad (2.8)$$

There follows a consequent recycling of the liberated chloride ions. The production of hydrogen chloride and hydrogen (H^+) or hydronium ions (H_3O^+), leads to increased acidity of the anodic area. The chloride and oxychloride compounds are more stable in such an environment and free to migrate further. The increased acidity also encourages further oxidation of the iron.

The exact manner in which chlorides break down the passive layer protecting the steel is not clearly known. There have been a number of suggestions by different researchers as to how the chloride ions actually depassivate iron under otherwise stable conditions (Foley, 1970, Shreir, 1979, Alvarez and Galvele, 1984, Leek and Poole, 1990). These are summarised as follows:

- Complex formation of iron halides on the surface. The overall process occurs with a chemico-adsorption reaction between a surface atom of the metal and the chloride. The complex can then pass into solution once a certain potential is reached. Once in solution the halide complex will dissociate and other more stable complexes (hydroxides) will be formed (Foley, 1970).
- Chloride ions are preferentially adsorbed in competition with oxygen and may displace passivating species, thus allowing for increased corrosion of the metal (Foley, 1970).
- The small size of the chloride ion gives it high penetrating power through the oxide layer (Shreir, 1979).
- Chloride ions result in local acidification thus destabilizing the anodic film at low pitting potentials. At higher pitting potentials local acidification is a necessity but not sufficient to induce pitting. Further anion adsorption is also required (Alvarez and Galvele, 1984).
- Breakdown in film passivity is a result of the destabilization of the film substrate bond with little or no chemical dissolution of the film (Leek and Poole, 1990).

However, the exact mechanism of chloride-induced corrosion is not essential for the general understanding of the influence of chlorides on corrosion of steel in concrete. Passivity should not be viewed as a complete protection of the underlying metal but rather as an extreme or limiting value of corrosion. The passive layer is normally in a continual state of breakdown and repair under normal conditions. The presence of chloride ions will contribute towards the breakdown of the passive layer while other anions such as OH^- are responsible for its stability and have inhibiting properties. There is a point therefore at which the concentration of aggressive ions overcomes the inhibiting ions and corrosion can initiate. This point is known as the pitting potential, below which passivity is maintained (Bockris *et al*., 1981).

2.3.3 ***Free vs. bound chlorides***

Not all of the chlorides in concrete are mobile and thus available for initiating or enhancing corrosion. Some of the chlorides are bound to the cement matrix as will be seen in the following sections. However, both free and bound chlorides usually exist simultaneously to maintain chemical equilibrium (Kropp, 1995).

2.3.3.1 ***Free chlorides***

These are the chloride ions dissolved in the concrete pore solution (Kropp and Hubert, 1995). They are termed water soluble chlorides. The concentration of free chlorides reduces with increasing concrete age due to effects such as chloride binding.

Early works suggested that only the free chloride contributes to the corrosion process but this has been disputed as will be seen in the next section. The free chloride content may be determined by one of the following methods:

- Pore solution expression (Tritthart, 1989, Glass *et al*., 1996)
- Leaching techniques (Arya *et al*., 1987, Castellote *et al*., 2001)
- Use of embedded Ag/AgCl electrodes (Elsener *et al*., 2003)

2.3.3.2 ***Bound chlorides***

Chloride binding can be defined as the removal of chloride ions from the pore solution through interaction with the binder matrix. All mineral cements bind chlorides to some degree and this strongly influences the rate at which chlorides penetrate into the concrete from an external source. Chlorides in concrete can be bound chemically through a reaction with C_3A (tricalcium aluminate) or C_4AF (tetracalcium aluminoferrite) to form calcium chloro-aluminates (Boddy *et al.,* 1999).

Chloride binding effectively removes chlorides from the transport process resulting in changes to the pore solution concentration, and thus the gradient driving ionic diffusion. Chloride binding may further influence chloride transport through partial blocking of pores due to the formation of calcium chloro-aluminates (Glass *et al*., 1997).

The nature of the concrete chemistry is important in determining the penetration of chlorides through concrete and thus the level of chlorides present at the steel. For example Glass *et al*. (1997) noted a variation in the order of binding efficiency with 65% slag replacement resulting in the greatest degree of chloride binding. The effects of cement extenders on chloride binding are graphically shown in Figure 2.5.

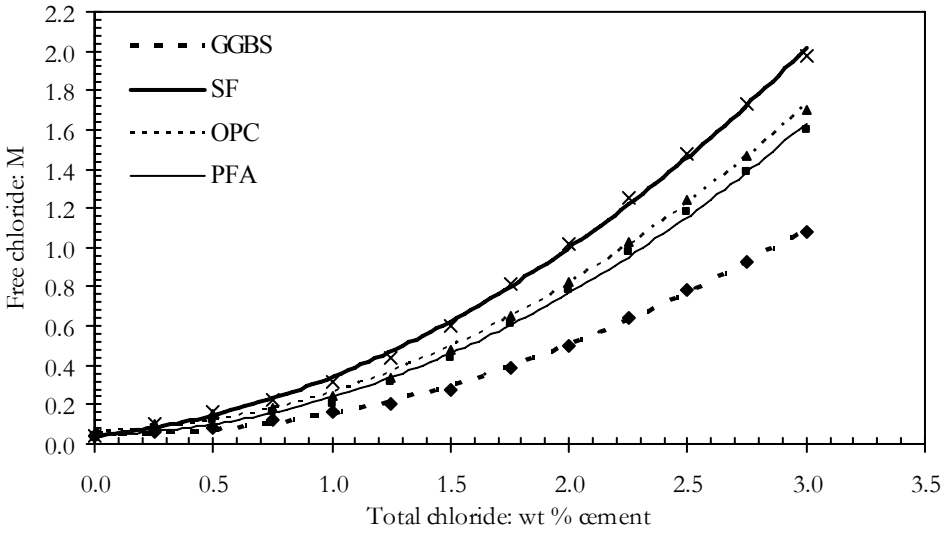

Figure 2.5: Chloride binding relationships dependant on binder type and total concentration (Glass *et al*., 1997)

what are the replacement levels?

2.3.3.3 ***Participation of bound chlorides in corrosion***

It has been postulated that only the remaining free chloride presents a significant corrosion risk. However, experimental evidence shows that bound chlorides may be released to participate in establishing a sustained corrosion process. Two mechanisms of releasing the bound chlorides have been proposed (Glass *et al*., 2000, Perez *et al*., 2000):

- The readily reversible nature of some of the chloride binding reactions. Thus bound chlorides may effectively maintain the acidity (low pH).
- The local acidification at the anode. Such acidification may promote the release of some bound chlorides. In this case the local chloride ion concentration would be increased above its initial value promoting further breakdown of the passive film. There is competition between two species: the ability of hydration products to resist a significant local drop in pH will inhibit corrosion initiation while at the same time the bound chlorides released by a small pH reduction may promote the establishment of a sustained corrosion process. The efficiency of these inhibitive mechanisms will depend on the magnitude of the pH reduction required to sustain corrosion compared to that required to dissolve the solid phases, and the kinetics of solid phase dissolution.

Therefore, bound chlorides may present a similar corrosion risk to free chlorides. The implications of this are that, while chloride binding retards chloride penetration, it also allows the build up of higher chloride contents that can increase the corrosion risk in some situations.

2.3.4 ***Chloride threshold level***

The chloride threshold level (or critical chloride concentration) is the concentration of chlorides necessary to break down the protective passive film on the reinforcing steel surface and initiate corrosion (Daigle *et al.*, 2004). It is the amount of chlorides that must be present at the steel surface before chloride-induced corrosion can be triggered. Knowledge of this value is important because it is a vital input parameter in service life design and service life prediction models.

The chloride threshold level is not a single value valid for all types of concretes, steels and environments, but is affected by a number of factors such as cover thickness, temperature, relative humidity, electrical potential of the reinforcement, chemistry of the binder, proportion of total chlorides to free chlorides and chloride to hydroxyl ion ratio (Nilsson *et al*., 1996). Since some of these factors change with time, it can be expected that the chloride threshold in a given concrete may also change with time.

Early works suggested that only the free chlorides contribute to the corrosion process and hence the free chloride content was regarded as the best expression of the critical chloride content. These proposals have been challenged by current studies (Glass and Buenfeld, 1997) as was mentioned in section 2.3.3.3. Therefore, a measure of the total chlorides in the concrete is probably a better representation when considering the chloride threshold.

Different approaches have been used to express the chloride threshold level including the following:

2.3.4.1 ***Free chloride threshold level***

This approach uses the free chloride (water soluble) content to represent the chloride threshold level, based on the assumption that the bound chlorides are relatively immobile and may not be transported to the steel surface (Yong and Song, 2007) i.e. it assumes that bound chlorides present no corrosion risk.

From literature, the chloride threshold level presented as a free chloride concentration ranges between 0.11 and 1.8 molar with w/b ratios ranging from 0.3 to 0.75 (Page *et al*., 1982, Petterson, 1995). Taking into account that bound chlorides also pose a corrosion risk, this method of presenting chlorides may an oversimplification.

2.3.4.2 ***[Cl^-]/[OH^-] ratio***

In this approach, the ratio between free chloride and hydroxyl ion concentration [Cl^-]/[OH^-] is used to express the chloride threshold level (Yong and Song, 2007). It also assumes that bound

chlorides are not a risk to corrosion, and that the hydroxyl ion concentration reflects the inhibitor content of the environment by sustaining the high pH of the pore solution.

This ratio expresses the ratio of aggressive to inhibitive ions causing corrosion initiation. Gouda (1970) described the relationship between chloride and hydroxyl ions by the equation:

$$pH = nLog[Cl^-] + K \quad (2.9)$$

where n and K are constants.

The ratio of $[Cl^-]/[OH^-]$, however, may not represent the critical threshold level well since it ignores the inhibitive effect of the cement matrix which may include a relatively denser hydration product layer on the steel surface (Page and Treadaway, 1982). Moreover, the ratio of $[Cl^-]/[OH^-]$ does not consider the dependence of chloride binding capacity on the hydroxyl concentration. The highly alkaline environment within concrete is caused primarily by the presence of metal hydroxides (KOH or NaOH) as mentioned earlier. The reduction of alkalinity may destabilize the chloro-aluminate, thus releasing bound chloride ions into the pore solution. However, an increase in the pH above 12.6 has been observed to produce a notable decrease in the level of the bound chloride (Tritthart, 1989, Glass *et al.,* 1997). Tritthart (1989) showed that an increase in the pH is accompanied by an increase in the $[Cl^-]/[OH^-]$ ratio at a fixed level of total chloride. This means that an increase in corrosion risk accompanies an increase in pH despite the inhibitive effect of hydroxyl ion or, that a $[Cl^-]/[OH^-]$ ratio is a poor representation of the threshold level.

2.3.4.3 ***Total chlorides***

The representation of the chloride threshold level as the total chloride (acid soluble) content is the most widely used approach. Most design codes use this approach to set maximum limits for chlorides. Table 2.1 gives a brief summary of some of these limits as required by different standards.

Table 2.1: Maximum total chloride content values set by ACI and BS standards

Type of element	*Maximum chloride content (%, cement)*			
	BS 8110	*ACI 201*	*ACI 357*	*ACI 222*
Prestressed concrete	0.10	-	0.06	0.08
Reinforced concrete exposed to chloride in service	0.20	0.10	0.10	0.20
Reinforced concrete that will be dry or protected from moisture in service	0.40	-	-	-
Other reinforced concrete	-	0.15	-	-

However, it must be realised that these limits are conservative and are not equivalent to the experimental chloride threshold values for total chlorides.

There still exists controversy on the minimum total chloride content that is required at the steel to initiate corrosion. Generally, a large scatter is found in the literature with results from 0.02 to 3.08% total chlorides by mass of binder (over two orders of magnitude) (Table 2.2). However, a conservative value of 0.4% total chlorides by weight of cement has been given by most authors (Daigle *et al*., 2004). The increased use of mineral extenders such as fly ash and slag also makes the prediction of the chloride threshold in concrete difficult.

Table 2.2: Some published total chlorides threshold values

Reference	*Binder type*	*Chloride threshold (% by mass of binder)*
Lambert *et al*., 1991	OPC, SRPC	1.0 - 3.0
Alonso *et al*., 2000	OPC	1.24 - 3.08
Alonso *et al*., 2002	various binders	0.73
Trejo *et al*., 2003	OPC	0.02 - 0.24
Scott, 2004	various binders	0.08 – 0.53

The large span of results might be due to reasons such as:

(i) Sample preparation, for example whether the chlorides were added during concrete mixing (admixed), type of chloride salt (e.g. CaCl, NaCl), binder type, type of steel, etc.
(ii) Testing methodology e.g. there is no defined line between potential to corrode (half-cell potential, E_{corr}) and actual progression of steel corrosion (corrosion current density, i_{corr}).
(iii) Different exposure conditions

All these make comparison of threshold values somewhat problematic, and hence the controversy. It would therefore be appropriate if the total chlorides threshold concentration was defined in such a way that it is binder-specific. Moreover, the variability in these values could be decreased if a standardised testing procedure is adopted.

The total chloride content may be determined using one of the following methods (Castellote *et al*., 2001, Glass *et al*., 1996):

- Potentiometric titration
- X-ray Fluorescence (XRF) spectrometry

2.3.5 ***Time to chloride-induced corrosion initiation***

2.3.5.1 ***Factors affecting time to chloride-induced corrosion initiation***

The time to corrosion initiation is dependent on the following factors:

- Chloride binding capacity of the binder
- Chloride threshold value
- Thickness of the concrete cover
- Resistance of cover zone to chloride ingress

(a) Effect of chloride binding on corrosion initiation

The effect of chloride binding on corrosion initiation is twofold: (1) the rate of chloride ionic transport in concrete is reduced since the amount of available mobile ions (free chlorides) is also reduced by the binding mechanisms and (2) the reduction of free chlorides in concrete results in lower amounts of chlorides being accumulated at the reinforcing steel layer (Hooton and Thomas, 2000).

The effect of cement extenders, and by inference chloride binding, on limiting the ingress of chlorides are provided by Tarek *et al*. (2002) in their examination of concrete after 15 years of exposure in tidal zones. For an assumed cover depth of 70 mm and a threshold value of 0.4% total chlorides by mass of cement, the time to initiation was found to be 22, 65 and 150 years for OPC, FA (10-20%), and slag (60-70%) respectively. Similar results have been obtained by Mangat *et al*. (1994) and Mackechnie and Alexander (1996). However, the increased time to corrosion initiation cannot only be attributed to chloride binding effects. Other effects such as the finer pore structure in the blended cements may also contribute to the longer time to corrosion initiation.

Even after corrosion has started, the rate at which it progresses will continue to be affected by binding as there is a much slower increase in chloride level which will in turn limit the increase in corrosion rate.

The effects of ground slag on chloride binding will be covered in the following sections.

Slags in South Africa can be of two types depending on the iron manufacturing process used. Both types are classified as latent hydraulic binders.

(i) ***Ground granulated blastfurnace slag (GGBS)***

This is a cementitious material formed when molten iron blast furnace slag is rapidly cooled by immersion in water. It is a granular product with very limited crystal formation and is highly cementitious in nature. South African GGBS has a typical Blaine fineness value of about 390 m^2/kg (Mackechnie *et al.*, 2003).

(ii) ***Ground granulated corex slag (GGCS)***

This is a cementitious material produced by the Corex process at the Saldhana steel plant in the Western Cape Province, South Africa (Corex is a registered Trade Mark of Voest-Alpine). It has been produced since 1999. GGCS is much finer than GGBS, with a Blaine fineness value of about 470 m^2/kg (Mackechnie *et al.*, 2003).

Comparing the Blaine finenesses, both GGBS and GGCS are more finely ground than OPC which typically has a Blaine fineness value of about 310 m^2/kg (Mackechnie *et al.*, 2003). Both GGBS and GGCS can either be interground with the clinker during the cement manufacturing process to make pre-mixed blended cements or intermixed with cement during the concrete mixing process. Table 2.3 shows typical oxide composition of South African OPC, GGBS and GGCS.

Table 2.3: Typical oxide analysis of OPC, GGBS and GGCS (% by mass, XRF analysis) (Mackechnie *et al.,* 2003)

Binder	*% Composition*									
	CaO	SiO_2	Al_2O_3	MgO	TiO_2	Fe_2O_3	MnO	K_2O	Na_2O	SO_3
OPC	67.2	22.3	4.4	1.01	0.22	3.4	0.08	0.56	0.21	0.58
GGBS	34.0	35.5	15.4	9.4	1.2	0.98	0.88	0.87	0.16	2.49
GGCS	37.2	30.8	16.0	13.7	0.51	0.87	0.09	0.35	0.12	3.19

Compounds that enhance the reactivity of slag include CaO, MgO and Al_2O_3 while SiO_2 reduces the reactivity. GGCS has higher CaO, Al_2O_3, and MgO concentrations than GGBS, and lower levels of SiO_2 (Mackechnie *et al.*, 2003). These differences in composition indicate that GGCS should have higher hydraulic reactivity than GGBS of equivalent fineness.

Effect of slag on chloride binding capacity of concrete

Chemical compounds similar to Calcium Silicate hydrate (C-S-H) are formed during the hydration reactions of ground slag, causing pore refinement (Jaul and Tsay, 1998). Ground slag is efficient in blocking the pores (fine-filler effect) since it reacts not only with $Ca(OH)_2$ and water to form C-S-H and calcium aluminates (Bakker, 1983). Thus, the formation of C-S-H gel results in the absorption of more chloride ions and blocking of diffusion paths. A higher content of C_3A in ground slag can also absorb more chlorides to form Friedel's salt (Leng *et al*., 2000). However, the chloride-binding capacity of ground slag can be reduced in the presence of sulphates in the binder or ingress from the environment (Leng *et al*. 2000, Luoa *et al.,* 2003).

In general, ground slag therefore decreases the free chlorides and increases the bound chloride content in concrete, which results in a lower probability of corrosion initiation of the reinforcing steel.

Effect of sulphides

Slag has a reducing character in its composition, containing manganese, iron, and other species in reduced states. The main contribution of its reducing power may be associated with the presence of soluble sulphides such as S^{2-}, HS^{-}, and S_n^{2-}, even though the total sulphide content of the slag may typically be less than 1% by mass. The reducing characteristics of granulated slag can influence the electrochemical potential of slag-OPC paste pore solutions (Pal *et al.*, 2002).

Sulphides affect the steel in two ways (West, 1980):

(i) The sulphides are oxidized to sulphate by the available oxygen thus depleting the oxygen concentration at the steel and creating a potentially reducing environment;

(ii) The sulphides form a precipitate of FeS on the steel surface thus affecting the formation of the passive layer.

Tromans (1980) also suggested that sulphides may be incorporated into the oxide layer thus reducing its ability to protect the steel. The depletion of oxygen in the presence of sulphides limits the formation of the passive layer on the steel surface, because the development of this layer is dependent on the availability of sufficient oxygen to supply the cathodic reaction. The embedded steel will therefore be more susceptible to corrosion and, with the availability of corrosive agents such as chlorides, time to corrosion initiation may be decreased.

The effect of sulphides therefore tends to downplay the improved overall concrete pore structure (mainly fine pore sizes). However, this effect may only be detrimental in the short term (depending on the sulphide content and the availability of oxygen). In the long term, the improved pore structure of the concrete due to incorporation of slag dominates and negligible corrosion rates may be noticed (Salvarezza *et al*., 1982).

(b) Effect of chloride threshold level on corrosion initiation

As was mentioned in section 2.3.4, the chloride threshold level is not a single value valid for all types of concretes, steels and environments. It is affected by a number of different factors such as cover thickness, temperature, relative humidity, electrical potential of the reinforcement and chemistry of the binder (Nilsson *et al*., 1996). These parameters vary from concrete to concrete and therefore corrosion initiation time will also have a similar variation among different binders.

The inclusion of cement extenders generally results in a lowering of the chloride threshold. The different performance of the cement extenders is attributed to the reduction in alkalinity and the presence of sulphides in the slag bearing materials (Scott, 2004). In a study using simulated pore solution, Scott (2004) found varying chloride threshold values for different binders as presented in Table 2.4.

Table 2.4: Variation of chloride threshold level with binder type (Scott, 2004)

Binder Type	*Concentration (% by mass of binder)*
Portland Cement (PC)	0.53
25/75 GGBS/PC	0.41
50/50 GGBS/PC	0.08
75/25 GGBS/PC	0.20
30/70 Fly ash/PC	0.36
50/43/7 PC/GGBS/silica fume	0.08

The low threshold values for the blended cements may be attributed to slow early hydration process leading to high short term concrete permeability. In the long term, the increased dense pore structure in these concretes may result in substantial decrease in corrosion rate or stifle the corrosion process.

(c) Effect of concrete cover on corrosion initiation

The concrete cover (or *covercrete*) may be regarded as a large transition zone with properties generally being inferior to those of the bulk concrete, particularly as the exposed surface is approached (du Preez and Alexander, 2004, Alexander and Mindess, 2005). It provides the initial resistance to degradation agents such as chloride ions. Therefore, the thickness, quality and condition of the concrete cover all have significant effects on the processes that lead to the corrosion of steel in concrete. The protective performance of the concrete cover is often further impaired by the presence of cracks.

A significant portion of the service life of a structure may be lost if the cover thickness is reduced (Torrent *et al*., 2007). On the other hand, excessively thick covers may result in wider flexural cracks which increase the penetrability of the cover. Therefore the cover thickness can only be increased up to a limit of about 80-90 mm (Neville, 1998). If this is unsatisfactory for the required durability, then the quality rather than the thickness should be increased.

2.3.5.2 ***Prediction of time to chloride-induced corrosion initiation***

The corrosion initiation period (t_i) for chloride-induced corrosion defines the time required for chlorides to accumulate at the steel level in sufficient concentration to break down the passive protective layer on the steel surface and thereby trigger corrosion process. No damage due to corrosion is assumed to occur during this period.

To predict chloride ingress in concrete structures the following salient issues should be considered (Daigle *et al.*, 2004):

(i) Concrete is a heterogeneous material that can include cracks.
(ii) Surface chloride concentration is known to vary with time.
(iii) Changing environmental conditions, such as temperature and humidity, affect the diffusion coefficient.
(iv) Hydration of cement paste is a chemical process that continues after the structure is put in service. This chemical reaction has an influence on the chloride diffusion coefficient.
(v) Interfaces between cement paste and aggregates influence chloride diffusion.

Prediction models based on consideration of diffusion alone are constructed around Fick's second law of diffusion. Fick's second law concerns the rate of change of concentration with respect to time and spatial position. For a semi-infinite homogeneous medium, and of whether the process is in steady state or not, the law may be stated as follows (Richardson, 2002):

$$\frac{\partial C}{\partial t} = D\frac{\partial^2 C}{\partial x^2} \tag{2.10}$$

where D is the apparent diffusion coefficient. The diffusion coefficient is not only a material property but also depends on the testing conditions.

With boundary conditions of:

$C_x = 0$ at $t = 0$ and $0 < x < \infty$
$C_x = C_s$ at $x = 0$ and $0 < t < \infty$
where C_x = chloride concentration at depth x at time t.
C_s = surface chloride concentration

Crank's error function solution (also called *Gauss error function*) of Fick's second law can be stated as follows (Richardson, 2002):

$$C_{x,t} = C_s\left[1 - erf\left(\frac{x}{2\sqrt{D_a t}}\right)\right] \tag{2.11}$$

where: $C_{x,t}$ = chloride concentration at the depth x at a given time t.

C_s = surface chloride concentration

D_a = apparent chloride diffusion coefficient

t = time of exposure

erf = error-function

However practical observations, especially in the case of intermittent impact of chlorides on concrete structures, have shown that the application of Fick's second law of diffusion entails certain conditions. Close to the surface, the concrete is exposed to a continuous cycle of wetting and subsequent evaporation (drying). Here the water carrying dissolved chlorides moves in and out; this contradicts the assumption for pure diffusion (Hunkeler, 2005) (Figure 2.6). Beyond this depth, diffusion is the decisive transport mechanism.

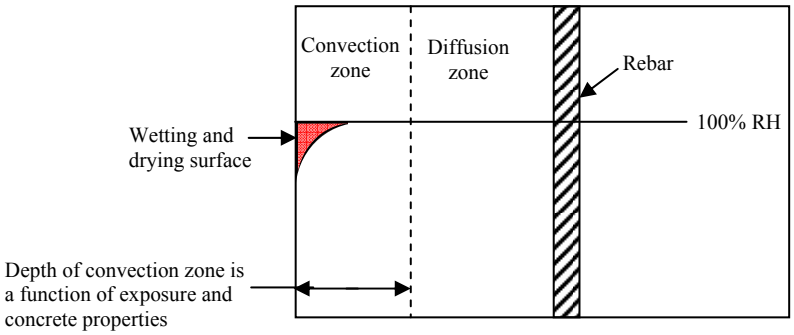

Figure 2.6: Convection zone in concrete (ACI Committee 365: LIFE 365, 2005)

Therefore, in order to describe the penetration of chlorides for intermittent loading with the error function solution of Fick's second law, the convection zone (Δx) was introduced by Gehlen (2000). Beyond the convection zone, the effect of dispersion and diffusion may then be described by a diffusion approach, for which the simple error function solution is again applicable. Instead of using the chloride concentration at the surface, the starting point of the calculation with the error function solution is thus the depth Δx where the concentration of chlorides is considered to remain constant over time (Figure 2.7).

$$C_{x,t} = C_i + \left(C_{\Delta x} - C_i\right).erf\left(1 - \frac{x - \Delta x}{2\sqrt{(t - t_{exp}).D_{(t)}(t)}}\right) \qquad (2.12)$$

where $C_{x,t}$ = chloride concentration at depth x at age t (wt.-% cement)

C_i = initial chloride background level (wt.-% cement)

$C_{\Delta x}$ = chloride content in depth Δx (wt.-% cement)

$D_{(t)}$ = time-dependent apparent diffusion coefficient (m^2/s)

t_{exp} = time until first exposure to chlorides (s)

t = concrete age (s)

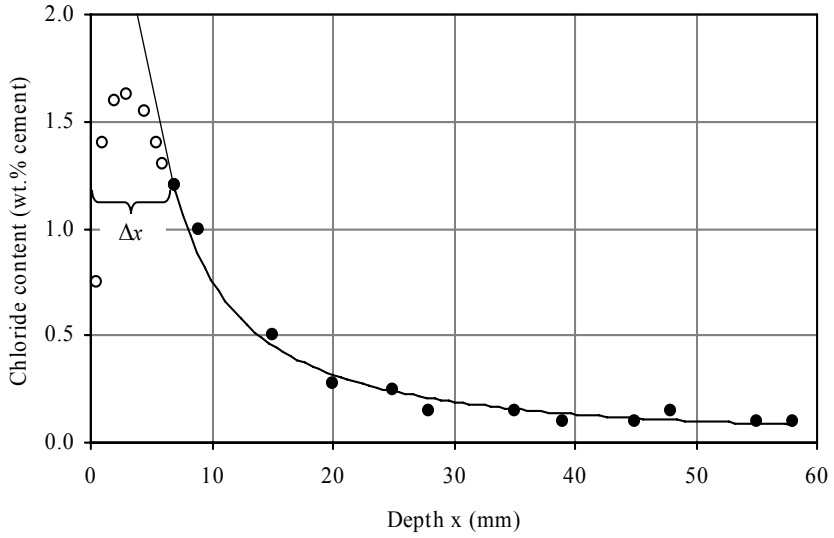

Figure 2.7: Typical chloride profile from splash zone (profile has been fitted to error function neglecting data points in the convection zone) (Hunkeler, 2005)

The time-dependent (*time-integrated*) diffusion coefficient ($D_{(t)}$) takes into account the decrease in chloride diffusivity with time due to effects such as continued hydration and chloride binding. This is described by the relation (Mackechnie, 1996):

$$D_{(t)} = D_o \left(\frac{t_o}{t} \right)^m \tag{2.13}$$

where D_o is the diffusion coefficient at reference time t_o (e.g. 28 days) and m is the aging coefficient (reduction factor). The value of the aging factor depends most significantly on the type of binder, and also on the rate of hydration and degree of drying.

The depth of the convection zone depends on (Tuutti, 1993):

- Drying and wetting time
- Time to capillary suction during wetting
- Difference in water pressure and
- Penetrability of the concrete to water

The convection zone can be estimated by:

(i) Chloride profiling in the laboratory

(ii) Using relative humidity measurements (Tuutti, 1993)

(iii) Using conductivity measurements in concrete under cyclic wetting and drying regime (Chrisp *et al*., 2002).

Some of the existing chloride-induced corrosion initiation prediction models are briefly discussed in the following sections.

(a) DuraCrete

DuraCrete is an acronym for *Dura*bility design of Con*crete* Structures (DuraCrete, 1998). It is a European design method for the durability of concrete that is explicitly based on performance, reliability, and a design service life, and recognizes that the service life of structures is a stochastic quantity that can be described in terms of probability (Siemes *et al*., 2000). It is follows the same principles (reliability and performance) as a structural design code and is based on realistic and sufficiently accurate definitions of environmental actions, material parameters for concrete and reinforcement, mathematical models for degradation processes and mechanical behaviour, performance expressed as limit states, and reliability.

The initiation period is determined using Fick's 2nd law of diffusion, with 28 day diffusion coefficients determined using the Rapid Chloride Migration (RCM) test.

An apparent drawback of the DuraCrete model is the need for a large amount of data to be able to quantify all the variables adequately for a specific kind of environment.

(b) ClinConc

ClinConc (acronym for *Chloride in Concrete*) is a Swedish performance-based numerical model developed by Tang (1996) and is used in the Scandinavian countries. It consists of two main procedures:

- Simulation of free chloride penetration through the pore solution in concrete using a flux equation based on the principle of Fick's law with the free chloride concentration as the driving potential, and
- Calculation of the distribution of the total chloride content in concrete using the mass balance equation combined with nonlinear chloride binding.

The ClinConc model uses free chloride as the driving force and takes chloride binding into account. However, since the ClinConc model needs numerical iterations for the binding effect, its practical engineering applications have been restrained due to the need of computation for numerical iterations. A more practical version has been proposed by Tang (2008). The model is also based on Fick's 2nd law of diffusion with the main input parameters being exposure conditions, concrete mix design and chloride diffusion coefficient obtained using the Rapid Chloride Migration (RCM) test.

(c) LIFE-365

LIFE-365 (2005) is a North American probabilistic computer-based simulation approach for service life prediction, and incorporates life-cycle cost functionality. It was developed by the ACI Strategic Development Council Consortium. In this model, it is appreciated that corrosion-induced damage can often be mitigated through numerous strategies including low concrete permeability, corrosion inhibiting admixtures, epoxy coated steel reinforcement, corrosion-resistant steel, application of waterproofing membranes or sealants or any combinations of these methods and materials. Each of these strategies has technical merits and costs, and the challenge is to select the proper combination of protection methods, at an acceptable cost, to achieve the desired result.

LIFE-365 model weighs the increased initial costs of specific corrosion protection systems against the potential extension of service life. The outcome is both the target service life being achieved and life-cycle costs optimised.

The analyses carried out within LIFE-365 can be split into four separate steps:

- Predicting the time to the onset of corrosion, commonly called the initiation period, t_i;
- Predicting the time for corrosion to reach an unacceptable level, commonly called the propagation period, t_p. The time to first repair, t_r, is the sum of these two periods (i.e. $t_r = t_i + t_p$)
- Determining the repair schedule after first repair; and
- Estimating life-cycle costs based on the initial concrete (and other protection) costs and future repair costs.

The following general user inputs are required for each RC structure or element:

- Geographic location
- Type of structure and nature of exposure
- Depth of clear concrete cover to the reinforcing steel, and
- Details of each protection strategy scenario such as water-cement ratio, type and quantity of mineral admixtures or corrosion inhibitors, type of steel and coatings, presence of membranes or sealers.

Like the previous models discussed, LIFE-365 is also based on Fick's 2nd law of diffusion to perform 1- and 2-dimensional finite difference calculations. In the process, the apparent chloride diffusion coefficient is adjusted for each time step in the calculations. However, contrary to the other models, it does not rely on laboratory or field measurements to obtain input parameters.

Many assumptions are made to simplify the model and hence the final solution only approximates the actual conditions. The calculated service life and life-cycle cost obtained using this model should therefore not be taken as absolute values.

(d) South African chloride ingress model

This is an empirical performance-based prediction model developed by Mackechnie (2001). It also predicts time to corrosion initiation for RC in a marine environment using Fick's 2nd law.

The model uses results of durability index tests (oxygen permeability, water sorptivity and, specifically chloride conductivity) to characterise early age concrete properties and then relate these to the potential durability performance of the material exposed to a range of marine environments. The environmental classification of the marine environments is based on EN 206-1 (2000), modified for South African conditions (Table 2.5) (Alexander and Beushausen, 2007).

The durability index tests are sensitive to changes in concrete pore structure and can therefore be used to characterise the early age material properties of the concrete in terms of the resistance of the cover concrete to ingress of deleterious fluids and ions. The early age properties are then used for comparative purposes and related to long term durability properties of the concrete in service. In short, the model is based on the relationship between early age properties, validated with long term chloride content data from marine concrete structures.

Table 2.5: South African environmental classes (after EN 206-1:2000) for chloride-induced corrosion

EN206 Class	*Description*
XS1	Exposed to airborne salt but not in direct contact with seawater
XS2a*	Permanently submerged
XS2b*	XS2a* + exposed to abrasion
XS3a*	Tidal, splash and spray zones Burrried elements in desert areas exposed to salt spray
XS3b*	XS3a* + exposed to abrasion

* These sub-clauses have been added for South African coastal conditions

The model uses the following procedure:

(i) The chloride conductivity index value of the concrete mix is obtained and used to predict the surface chloride concentration and long tern chloride diffusion coefficients.

(ii) Fick's 2nd law is the applied to predict the chloride profile

(iii) Using a nomogram, an estimation of the time to corrosion initiation is made based on the assumption that corrosion initiation occurs when the chloride concentration at the rebar level reaches 0.4% by mass of binder.

2.4 Corrosion propagation

When corrosion agents (O_2, CO_2, H_2O, Cl^-) continue to be available at the corrosion sites (anode and cathode) after corrosion initiation, corrosion may proceed into the propagation stage. Corrosion propagation is characterised by active corrosion and may lead to generation of cracks, delamination, and spalling of concrete cover due to expansive corrosion products (Yoon *et al*., 2000). Conventionally, it is taken that corrosion rates below 0.1μA/cm^2 characterise a passive corrosion state, whereas rates above this value characterise active corrosion (Gonzalez *et al.,* 1995, Alonso *et al.,* 2002) i.e. corrosion rate of 0.1μA/cm^2 is taken as the transition point from passive to active corrosion.

2.4.1 Factors affecting corrosion propagation of steel in concrete

After corrosion initiation, the rate at which corrosion progresses due to exposure to corrosion agents depends on several factors including temperature, w/b ratio, binder type, presence of cracks, concentration of the chemicals, duration and condition of exposure, and the chemical resistance of concrete.

This section focuses is on factors that affect corrosion rate due to chloride-induced corrosion including, among others, presence of cracks on the concrete surface, w/b ratio and the effect of slag.

2.4.1.1 Effect of cement extenders on corrosion propagation

Apart from having an influence on corrosion initiation, mineral cement extenders such as slag, fly ash and silica fume also have a profound effect on the rate at which corrosion progresses (Mangat *et al*., 1994, Mackechnie and Alexander, 1996). Extensive research has been done on the use of cement extenders and as a result, a better understanding of the influence of cement extenders on the corrosion rate has been developed.

Song and Saraswathy (2006) reviewed previous studies on the corrosion resistance of reinforced steel in concrete with ground granulated blast-furnace slag and concluded that replacement of cement by 40% slag has no significant influence on corrosion rates of rebar in concrete. At 60% slag content the corrosion rate is significantly reduced. Hence, an increase in slag proportion decreases the rate and amount of corrosion of reinforcement in slag concrete.

2.4.1.2 ***Effect of relative humidity on corrosion rate***

Moisture content in concrete is an important factor for both corrosion initiation and its progress. It highly influences corrosion initiation time as it influences the intrusion of both oxygen and carbon dioxide but is an important pre-requisite for the penetration of chlorides by diffusion (section 2.3.5.2), (Hunkeler, 2005). In the propagation period, the rate of corrosion is also influenced by moisture condition of the concrete.

The corrosion rate is slow in dry or saturated condition, but at intermediate moisture contents, moisture acts as an electrolyte, and such moisture contents also allow the intrusion of oxygen to the corrosion process (DuraCrete, 1999). In dry conditions, there is no moisture to support the corrosion process whereas in saturated conditions, movement of oxygen through the concrete to the steel level may be significantly impaired because oxygen does not readily dissolve in water. A corrosion cell can therefore not occur if the concrete is too dry to serve as an electrolyte or too wet (saturated) to allow ingress of oxygen. Corrosion activity is most vigorous at relative humidity (RH) values above 80%. According to Richardson (2002), chloride induced corrosion is at a maximum when the RH within the concrete is around 90-95%.

There appear to be two main inter-related mechanisms for controlling the corrosion rate of steel, both dependent upon the relative humidity of the concrete. The movement of O_2 from the atmosphere to the surface of steel is a function of the diffusion coefficient (the ease with which O_2 can move through concrete) and the depth of the steel. The diffusion coefficient is in turn affected by both the w/b ratio (through the permeability of the concrete) and the relative humidity of the concrete. The movement of O_2 through concrete is significantly reduced by an increase in the proportion of water-filled voids. The O_2 diffusion coefficients for two w/b ratios of cement paste at various RH are provided in Figure 2.8.

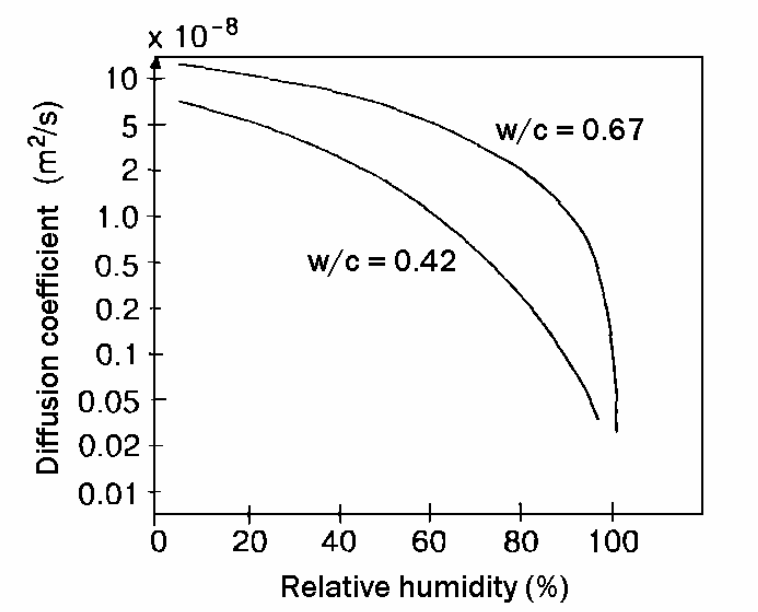

Figure 2.8: Influence of w/c ratio and RH on the diffusion coefficient for O_2 (Bentur *et al*., 1997)

The moisture condition (or relative humidity) of concrete is therefore an important factor in controlling corrosion rate. It mainly affects the availability of oxygen (which is required to support corrosion) depending on whether the concrete is dry or saturated. In between, there is an optimum RH range for chloride induced corrosion.

2.4.1.3 ***Influence of temperature on corrosion rate***

The significance and influence of temperature as a factor in steel reinforcement corrosion rate is evaluated by means of the universal dependence of chemical reactions on surrounding temperature. According to this, the rate of chemical reaction is accelerated as the surrounding temperature is increased. But experimentally it has been found that dependence of the rate of steel reinforcement corrosion on the surrounding temperature is more complex. This complexity has been shown by an accelerating effect up to a temperature of 40°C followed by an inhibiting effect occurring above this temperature. The main cause of this phenomenon is attributed to the decreasing oxygen solubility in the pore solution when the temperature is increased (Zivica, 2003).

A rise in temperature may result in a twofold effect: the electrode reaction rates are generally increased, and the oxygen solubility is increased (up to about 40°C) resulting in an increase in the rate of corrosion (Mazer, 1965). If the situation is conducive for corrosion to take place, the corrosion rate is increased by high temperature and high humidity (Uhlig, 1983). Maslehuddin (1996) also showed that corrosion rate is affected by temperature gradients at temperatures between -25 and 40°C.

2.4.1.4 ***Influence of water/binder ratio and binder content on corrosion rate***

The water/binder (w/b) ratio affects the corrosion characteristics of the concrete primarily by shaping the pore structure. High w/b ratio has a negative effect on steel reinforcement corrosion mainly due to increased permeability of concrete. The effect is due to faster diffusion of chloride ions to the steel level, easier oxygen penetration and lower electrical resistivity of the concrete (Petterson, 1997).

For concrete in a moist environment, the cathodic reaction rate depends on the availability of oxygen and the corrosion rate may therefore be limited by the cathodic reaction. With a decrease in w/b ratio, the quantity of oxygen decreases due to decreased concrete permeability. Therefore, decreasing the w/b ratio suppresses the cathodic reaction leading to a decrease in the corrosion rate. In addition, the concrete resistivity increases with a decrease in the w/b ratio. Moreover, corrosion rate may also be controlled by the alkalinity, which is higher in concrete that has a lower w/b ratio.

Corrosion rates for 12 mm deformed steel cast in concrete, with a cover of 10 mm, and three different w/b ratios and cement contents, were examined by Mangat and Molloy (1992). The specimens were exposed to cyclic periods of wetting and drying after 14 days air curing. The results are provided in Table 2.6.

Table 2.6: Influence of w/b and cement content on corrosion rates (Mangat and Molloy, 1994)

w/b	*Cement* (kg/m^3)	i_{corr} (uA/cm^2)	Cl^- (*% mass cem.*)
0.45	430	0.13	1.4
0.58	430	0.65	2.0
0.58	330	0.62	1.73
0.58	530	0.52	1.21
0.76	430	2.16	2.3

It is evident that w/b ratio had a more significant impact upon the corrosion rate of steel in concrete than cement content. The highest corrosion rate was observed in the 0.76 w/b ratio with the accompanying highest chloride concentration while the lowest corrosion rate of 0.13 $\mu A/cm^2$ was found to occur in the w/b 0.45 sample despite having higher chloride content than the 0.58 w/b with 530 kg cement. The effects of the material are thus more significant than simply limiting the chloride ingress. The cement content was shown not to significantly affect the corrosion rate.

The influence of w/b ratio on corrosion rate is therefore significant and should be taken into account at the concrete mix design stage if the RC structure will be exposed to aggressive environments during its service life. For less aggressive environments, careful selection of w/b ratio may also be successfully used to limit corrosion.

2.4.1.5 ***Influence of concrete cover thickness on corrosion rate***

Concrete cover thickness influences mainly the ingress of chlorides and oxygen into the concrete. The quality of the concrete cover especially with respect to its penetrability determines the ease of ingress of the chloride ions. Reduction of concrete cover reduces the travel path for the chloride ions and oxygen to reach embedded steel (Hawkins and McKenzie, 1996).

The effects of cover on the diffusion of O_2 are shown in Figure 2.9 depicting that an increase in cover depth from 20 to 50 mm results in a reduction in the availability of O_2 at 60% RH (Bentur *et al*., 1997). Thus the coupled effect of an increasing cover depth and a shift in RH from 60 to 80% results in approximately twice the decrease in the availability of O_2. The increased cover depth is also likely to minimize the influence of the external drying at the depth of the steel thus sustaining a fairly high RH.

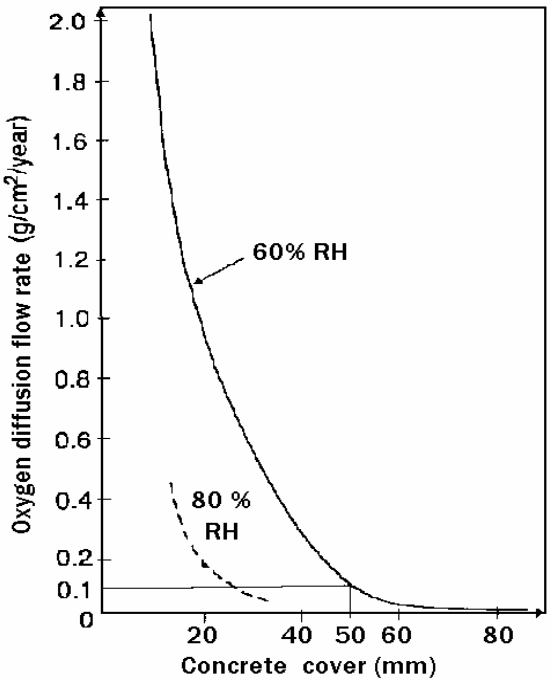

Figure 2.9: Effect of concrete cover on the diffusion of O_2 (Bentur *et al*., 1997)

Concrete cover therefore affects the corrosion rate mainly by governing the travel path of the corrosion agents (oxygen, moisture, chlorides). Just like w/b ratio, concrete cover may also be used to inhibit corrosion. In fact, when w/b ratio, cover, binder type and binder content are

carefully chosen, corrosion may be significantly inhibited during the service life of a RC structure. In general, a small concrete cover may be used for a high quality (less penetrable) concrete while the same cover thickness may not apply for a lower quality concrete cover.

2.4.1.6 ***Influence of cracks on corrosion***

Concrete is essentially waterproof in an uncracked state when properly placed, compacted, and adequately cured. However, as it gradually loses its water-tightness in the course of its service life due to the formation of cracks, concrete becomes vulnerable to deterioration by corrosion of reinforcement.

Two forms of cracks are of interest when evaluating the condition of a reinforced concrete structure; those present before the onset of corrosion which might assist the corrosion processes, and those produced as a direct consequence of corrosion. This study is interested in the former.

In extreme cases, cracks may affect the structural integrity of the concrete member. However, in most instances, cracks do not affect the load-carrying capacity of the concrete structure but may adversely affect its durability by providing easy access to aggressive agents, especially chloride ions in marine environments (Transportation Research Circular E-C107, 2006). The effects of cracks in concrete cover vary not only with their effective depth, but also with their width, frequency and orientation (relative to the steel reinforcement). These factors will be explored in this section.

(e) Causes of cracks in concrete

Cracking is an inherent feature of concrete and the effects may range from trivial to catastrophic. Cracks in RC structures are inevitable and arise during all stages in the life of a concrete structure (Ismail *et al*., 2004). Reinforced concrete elements are therefore usually designed on the assumption that cracking should take place under standard loading conditions (Nilsson and Winter, 1985, Nawy *et al*., 2001). Although this study focuses on macroscopic loading cracks, a crack network exists in concrete with contributions from various sources. These will be briefly reviewed.

While cracks may develop in concrete from a variety of causes, the underlying principle cause is the relatively low tensile strength of concrete. Concrete is a quasi-brittle material with a low capacity for deformation under tensile stress. Cracking occurs when the applied tensile stresses exceed the tensile strength of the concrete.

ACI 201 defines a crack as a *complete or incomplete separation of concrete or masonry, into two or more parts, produced by breaking or fracturing*. Cracks may appear at the surface, but may not go through the whole concrete depth. In concrete, microcracks already exist due to its inhomogeneous nature as a composite material. Other cracks develop due to temperature and moisture gradients, service loads (Pedro *et al*., 2004) or deterioration mechanisms such as reinforcement corrosion, frost action and alkali aggregate reaction (Jacobsen *et al*., 1998).

Table 2.7 summarises the possible causes of cracks in concrete as summarised by the Transportation Research Circular E-C107 (2006).

Table 2.7: Possible causes of cracks in concrete
(Transportation Research Circular E-C107, 2006)

Before Hardening		*After Hardening*			
Constructional movement	*Plastic*	*Physical*	*Chemical*	*Thermal*	*Structural*
• Formwork movement • Sub-grade movement	• Early Frost damage • Plastic settlement • Plastic shrinkage	• Shrinkable aggregates • Drying shrinkage • Crazing	• Reinforcement corrosion • Alkali-Aggregate Reaction • Carbonation	• Freeze/Thaw cycles • Early thermal contraction • Temperature variations	• Accidental overload • Creep • Design loads

(f) Autogenous healing of cracks in concrete

The term 'autogenous healing' (also referred to as *self-healing*) refers to the ability of the cementitious material to heal cracks in concrete. It involves both physico-chemical and mechanical processes. The following physical, chemical, and mechanical processes have been suggested to be the main reasons for the autogenous healing of concrete (Edvardsen, 1999):

(i) Swelling and hydration of cement paste
(ii) Precipitation of calcium carbonate crystals
(iii) Ettringite formation
(iv) Blocking of flow path by impurities in water and
(v) Blocking of flow path by the concrete particles (debris) broken from the crack surface due to cracking.

The most significant factor which influences autogenous healing is the precipitation of calcium carbonate ($CaCO_3$) (Schiessl, and Reuter, 1992, Schiessl and Edvardsen, 1993). However, regardless of the origin, self-healing leads to the sealing of cracks thus improving the durability, permeability and mechanical properties of concrete (Edvardsen, 1999).

To a considerable degree, the autogenous healing process is influenced by the crack width and the prevailing water pressure, whereas the type of binder, aggregate, and filler and the hardness of the water are of a lesser influence (Edvardsen, 1999, Reinhardt and Joss, 2003). Smaller cracks are therefore more likely to heal, and at a faster, than larger ones.

The occurrence and benefits of autogenous healing are especially significant in the reduction in concrete penetrability and hence improving the protection of the embedded steel from corrosion (Neville, 2002).

An important practical question is: what is the maximum crack width that can be closed by autogenous healing? Various researchers have reported different maximum crack widths for which autogenous healing is possible but this is not surprising because the testing conditions also vary. The following may vary from one experiment to another:

- How the cracks were produced e.g. by shrinkage, application of tension (usually flexural), or by direct tension
- The age at which the cracks were opened
- Whether healing took place in static water or flowing water
- The presence or not of a water or not
- Type of water used e.g. fresh, sea water, lime-saturated water.
- The material undergoing the autogenous healing (concrete or mortar)

The combinations of these conditions are numerous, so that generalizations about the maximum width of cracks that will heal are not possible. Table 2.8 presents some of the findings of various researchers.

Table 2.8 : Some studies on autogenous crack healing (Summarised from Neville, 2002)

Reference	*Results*
Wagner (1974)	A 0.33 mm crack (in a mortar lining of metal pipes) was still open after 30 days' immersion in city water, but healing had taken place below the surface.
Vennesland and Gjorv (1981)	Corrosion was observed in all RC blocks with crack widths of 0.4 mm or more
Gautefall and Vennesland (1983)	Specimens with cracks more than 0.6 mm wide were susceptible to corrosion attack but this did not happen when the cracks were less than 0.4 mm wide Immersed in seawater (ample oxygen was available at a separate cathode, which was remote from the anode)
Edvardsen (1999)	25-50% of 0.20 mm cracks wide healed completely after 7 weeks of water exposure. The proportion of cracks closed depended on the water pressure

However, regardless of the maximum crack width at which autogenous healing is possible, cracks up to a certain width in RC are inevitable and acceptable, hence the concept of acceptable or allowable crack widths. The next section will cover this.

(g) Allowable crack widths

The maximum crack width considered acceptable depends on the type of structure, the location within the structure, the exposure conditions, and the consequences of excessive cracking (Park and Paulay, 1975, Haldane, 1976, Ismail *et al*., 2004).

Some concrete design codes limit the surface transverse crack widths to control corrosion of steel in concrete (ACI Building Code, 1995, British Standards Institution (BS 8110: Part 1-1997, Japan Society of Civil Engineers (JSCE) 1986). On the contrary, European design code (CEB, 1989) recommends that the limitation of crack widths is no means to avoid the attack to the reinforcement in the case of severe chloride attack to horizontal concrete surfaces. This may be due to the ponding effect of the chlorides on the concrete surface, and hence faster ingress of the chlorides into the concrete.

To ensure durability, maximum crack width in a corrosive and aggressive environment may need to be considerably small. Results of exposure tests and site inspections confirm that within a common range of crack widths (up to 0.4 mm), the influence of the transverse crack on the corrosion rate of steel bars is relatively small (CEB/FIP model code, 1992). Hence most codes adopt a crack width of 0.4 mm as a threshold value.

At this point, it must be mentioned that crack widths are inherently subject to wide scatter (Nejadi, 2005) even in carefully monitored laboratory tests, and are influenced by shrinkage and other time-dependent effects.

In designing a concrete structure against corrosion, several codes and specifications provide equations to predict the maximum crack widths that are expected to result from the loads and stresses carried by the structure e.g. ACI 318, 1995 (Table 2.10). On the other hand, some codes limit crack widths by specifying the maximum allowable steel stress at cracked sections for different bar diameters and bar spacing e.g. the Australian Standard AS 3600 (2001) (Table 2.9). Others give the designer both the option of predicting the maximum crack width and also limiting the steel stress e.g. British Standards Institution (BS 8110: Part 1, 1997 and BS 5400 Part 4, 1990) (Table 2.10).

Table 2.9: Maximum steel stress for tension or flexure to limit cracking (AS 3600, 2001)

Nominal bar diameter (mm)	*Max. steel stress (MPa)*

10	360
12	330
16	380
20	240
32	160

Table 2.10: Examples of crack width prediction formulae

Code/Specification	*Crack width prediction equation* (W_{max})
ACI 318 (1995)	0.132z
BS 8110: Part 1 (1997) and BS 5400: Part 4 (1990)	$\frac{3a_{cr} \in_m}{1+2\left(\frac{a_{cr}-c}{h-d_c}\right)}$

where

a_{cr} = distance from crack to nearest bar surface which controls width

$\in_m$ = calculated strain at the level where cracking is considered, allowing for the stiffening effect of the concrete in the tension zone

h = overall depth of section

d_c = depth of concrete in compression

c = cover to outermost reinforcement

z = $f_s(cA_e)^{1/3}$

A_e = effective area of concrete

It appears that there is no single answer to the question of permissible crack widths. Complex inter-relations among properties of the concrete cover, exposure conditions, and designed service life of the structure should be used to determine the crack widths that can be tolerated without significant corrosion.

(h) Effect of cracking on chloride ion penetration

Cracks in concrete may cause localised chloride ingress and hence localised steel corrosion. Mass transfer of corrosion species in cracked concrete, e.g. chloride ion diffusion, has been shown to increase after cracking of concrete (Sagues and Kranc, 1998).

Transverse crack width (with respect to the reinforcing bar orientation) in the tension zone of about 0.1 mm has been interpreted to allow proportionately greater penetration of chlorides in the vicinity of the cracks due to microcracking internal to the concrete near the bar. This may be caused by bond-related transfer of tensile strain within the concrete adjacent to the

reinforcement or by temperature or other strains (Bentur *et al.*, 1997). The damage decreases with distance from the (transverse) macrocrack implying non-homogeneity in concrete permeability (Goto 1971, Beeby 1978, Schiessl 1998).

Mohamed *et al*. (2003) carried out both short term accelerated laboratory and long term exposure tests on mortar specimens prepared using OPC, blastfurnace slag and fly ash at w/b ratios of 0.3 and 0.5. Single surface crack of width 0.3 mm was used in the specimens. They found that at a constant surface crack width of 0.3 mm, the w/b ratio affects the chloride ingress. Figure 2.10 shows the chloride ingress trends for studies done by Mohamed *et al.* (2003). The increase in the chloride ion concentration for the concrete having w/b ratio of 0.5 compared to that of 0.3 can be attributed to crack healing at the smaller crack. For crack healing to occur, there must be unhydrated cementitious material in the concrete. This may occur if the w/b ratio is low. In the presence of the crack, moisture is absorbed from the surrounding, facilitating further hydration. It is the hydration products that partly seal the crack hence reducing its penetrability to chloride ions.

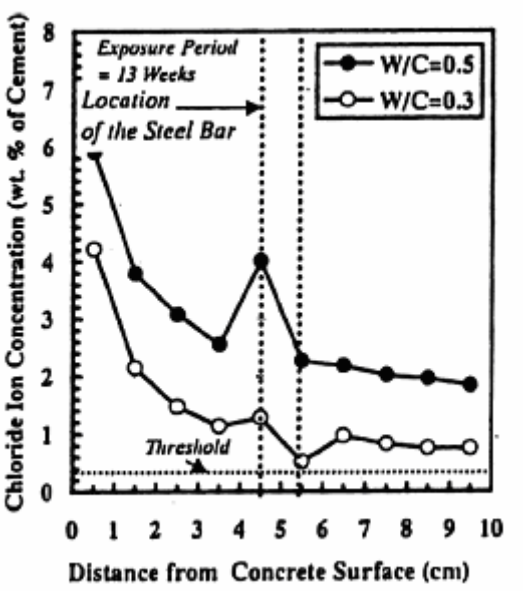

Figure 2.10: Chloride ion profile across a constant surface width crack of 0.3 mm (Mohamed *et al.,* 2003)

(i) Effect of crack width on corrosion rate

There is no general agreement on the relationship between crack width and corrosion. Bentur *et al*. (1997) indicated that for two reinforced concrete specimens that differ only in crack width, the time required to initiate corrosion is shorter for one with wider cracks, but the corrosion rates are not significantly influenced by crack width. However, Beeby (1983) and Arya and Wood (1995) suggest that there is no direct relationship between crack width and corrosion rate. They consider more important factors to be the following:

(i) Crack properties, for instance whether the crack is active or dormant
(ii) Concrete and steel properties, whereby low permeability of the concrete will limit ionic transport, high moisture contents will limit oxygen ingress and increased strength leads to better bond and less slip at the steel-concrete interface, and
(iii) Service environment.

Pettersson (1996) investigated the influence of crack width on corrosion process using different mix proportions and found that when the crack widths remained relatively small (<1.0 mm), they had little impact on the corrosion process; however, larger cracks (>1.0 mm) increased the corrosion rate.

Francois and Maso (1988) initiated a long-term study on reinforced concrete beams loaded in three-point flexure. The generated crack widths were between 0.05 and 0.5 mm. They concluded that chlorides penetrate rapidly through cracks.

Suzuki *et al*., (1990) support the argument of limited effect of crack width on corrosion rate, though they note some early-age differences in corrosion rate based on crack width, but these decrease with time due to crack healing. The w/b ratio was found to have a more significant impact on corrosion rate than crack width.

In a study by Scott (2004) on South African materials, different binder types (OPC, Slag and Silica fume) were used. Surface crack widths of 0.2 mm and 0.7 mm were introduced in the concrete specimens by the slipping of plain round bars. 5% NaCl solution was used while the w/b ratio was kept constant at 0.58. Two different concrete covers (20 mm and 40 mm) were used. From the study, it was concluded that binder type, crack width and concrete cover thickness all affect the corrosion rate of the steel. It was also found that for an OPC concrete, at a constant crack width, the decrease in the concrete cover results in a significant increase in corrosion rate compared to concrete made with blended cements. Generally, the corrosion rate increases as the concrete cover thickness decreases (Table 2.11). The same trend was observed for the 0.7 mm crack width using the same cover thicknesses of 20 mm and 40 mm. The effect of concrete cover depth can therefore be deduced to have a profound effect on corrosion rate of OPC concretes, other factors being constant.

It can be depicted that for a constant concrete cover, increasing the surface crack width for a given concrete cover results in higher corrosion rates. This is expected because, at a constant cover, increasing the surface crack width results in a greater steel surface being exposed, assuming the crack is wedge-shaped. This raises serious concerns relating to corrosion rate

inter-study comparisons that are done taking into consideration only the similarity in surface crack width and disregarding the influence of cover depth amongst other factors.

Table 2.11: Influence of crack width and cover on corrosion rate (Scott, 2004)

Binder type	*Corrosion rate ($\mu A/cm^2$)*			
	0.2 mm crack width		*0.7 mm crack width*	
	20 mm cover	*40 mm cover*	*20 mm cover*	*40 mm cover*
100 % CEM I (OPC)	2.65	1.20	3.23	1.48
50/50 GGBS/CEM I	0.39	0.35	0.51	0.53
30/70 Fly ash/CEM I	0.64	0.39	0.71	0.50
50/43/7 CEM I /GGBS/Silica fume	0.67	0.59	1.12	1.03

Add my results summary here

(j) Effect of crack frequency on corrosion rate

Crack frequency refers to the number of cracks present on the concrete surface per given length. Current theory of crack formation agrees that where many surface cracks exist in concrete, crack frequency (or *crack density*) is more important than crack width.

A study by Arya and Ofori-Darko (1996) confirmed this after conducting tests by varying the crack frequency from approximately 0 to 20 cracks per metre length. The equally spaced parallel-sided cracks had a constant width and depth of 0.3 mm and 40 mm respectively. A concrete cover of 42 mm was used for all the specimens. Two series of tests were conducted using two different NaCl concentrations of 3% and 5%. The concrete had a w/b ratio of 0.65. Figure 2.11 shows a plot of the cumulative mass loss of the reinforcement steel against time. It is clear that the corrosion rate increases with the increase in the crack frequency. They also concluded that while cracks may accelerate corrosion initiation, the subsequent rate of corrosion may be minimal for transverse cracks.

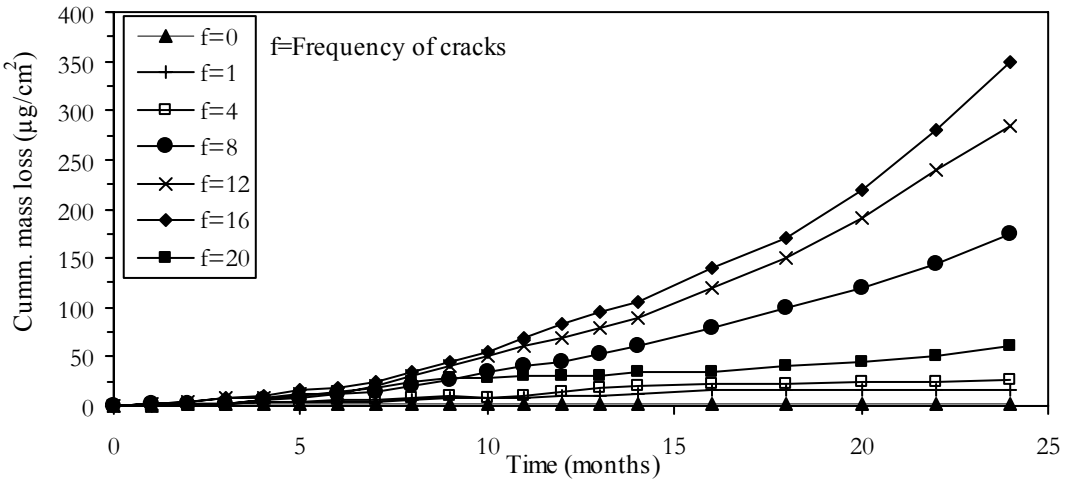

Figure 2.11: Effect of crack frequency on cumulative mass loss due to corrosion (Arya and Ofori-Darko, 1996)

The cumulative mass loss (Figure 2.11) gives an indication of the corrosion rate of the steel. It can therefore be concluded that the corrosion rate increases with increasing crack frequency. This can be attributed to the increase in the permeability of the concrete, and hence ease of chloride ion ingress into the concrete. It must be noticed that the specimens with the highest crack frequency of 20 did not correspond to the highest corrosion rate. The crack frequency of 16 may be the optimum under the given set of experimental conditions above which corrosion rate decreases.

(k) Effect of crack orientation on corrosion rate

Orientation of cracks with respect to reinforcement is an important factor influencing crack-induced corrosion. According to their orientation, cracks can be grouped as either coincident or intersecting.

Cracks along the line of the reinforcement are called coincident or longitudinal. They can be induced by various mechanisms including plastic settlement, plastic shrinkage and bond failure. With regard to chloride-induced corrosion, this type of cracking is extremely dangerous, since chlorides, moisture, and oxygen can easily penetrate to the embedded steel and attack large areas of steel in the corrosion process.

Cracks across the reinforcement are termed intersecting or transverse. In this case, the cathodic areas of reinforcement mostly occur in the crack-free regions. Therefore, moisture and oxygen that enter through the cracks do not significantly affect the rate of corrosion (Arya, 1995). But not according to my results. Criticise.

Longitudinal cracking is more likely to result in higher corrosion rates than intersecting cracks (Beeby, 1983, Arya and Wood, 1995, Arya and Ofori-Darko, 1996, Bentur *et al.,* 1997). However, for concrete in service, transverse cracks are more frequent in tensile- stressed areas of a RC structure than longitudinal cracks. The latter are more associated with corrosion cracks along the longitudinal reinforcement due to the large volume (or expansive nature) of corrosion products.

2.4.1.7 ***Effect of cyclic wetting and drying on corrosion rate***

The moisture content of concrete has a direct influence on durability as it governs the amount of oxygen and moisture available at the reinforcing steel level, and the magnitude of the capillary suction forces, which dictate the rate of penetration of water (McCarter and Watson, 1997). Cyclic wetting and drying of concrete causes continuous moisture movement through concrete pores. This cyclic action accelerates durability problems by subjecting concrete to the accumulation of harmful materials such as sulphates, alkalis, acids, and chlorides.

Several factors can affect the extent to which chlorides penetrate into concrete through cyclic wetting and drying. For structures exposed to cyclic wetting and drying, absorption and diffusion are the two most significant transport mechanisms that govern chloride ingress (Nanukuttan *et al*., 2008).

Chloride ingress is also strongly influenced by the sequence and duration of cyclic wetting and drying. Specifically, the degree of dryness and therefore the surrounding drying conditions are very important (Hong and Hooton, 1999). The degree of drying influences the extent to which the chlorides travel into the concrete by wick action. To investigate the effect of cycle period on chloride ingress into concrete, Hong and Hooton (1999) carried out experiments by subjecting concrete samples (made with w/b ratio of 0.40 and cured in a saturated $Ca(OH)_2$ solution for 28 days) to two wetting and drying regimes viz 1-day and 3-day cycle periods with 1.0 M NaCl solution at 23 ^{o}C for 120 days or 1 year . The results showed that both the duration of wetting/drying and the number of cycles affect the depth of chloride ingress into concrete (Figure 2.12 and Figure 2.13).

From these figures, it can be seen that a 3-day cycle results in a higher chloride concentration than a 1-day cycle up to depths of approximately 14 mm from the concrete surface. However, it is also clear that for a given cycle regime (1-day or 3-day), the chloride ion concentration at a given depth of the concrete cover increases with an increase in the number of cycles. It can therefore be concluded that both the cycling duration and the number of cycles affect chloride ingress into concrete keeping other factors constant.

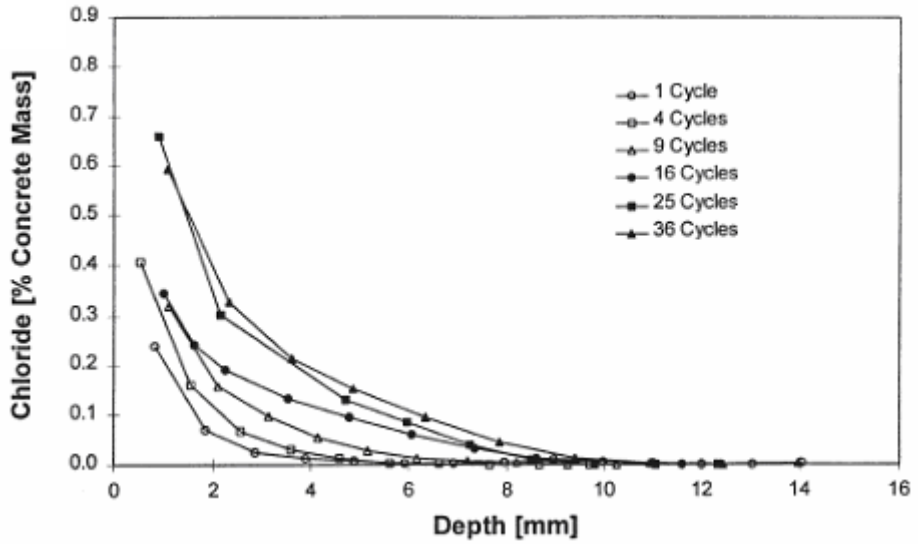

Figure 2.12: Chloride profiles for concrete with 25% slag, 1-day cycle for 120 days (Hong and Hooton, 1999)

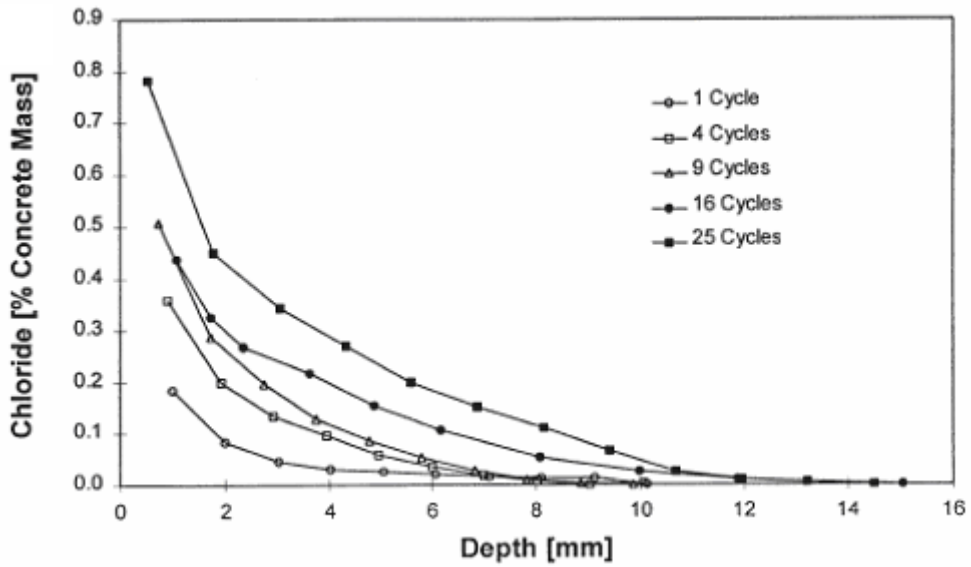

Figure 2.13: Chloride profiles for concrete with 25% slag, 3-day cycle for 120 days (Hong and Hooton, 1999)

Dry or partially dry concrete when exposed to salt solution absorbs the salt solution by capillary suction. The concrete absorbs the salt solution until saturation. Drying to a greater depth allows subsequent wetting to carry the chlorides deeper into the concrete, thus speeding up the penetration of chloride ions, (Neville, 1996). If the concrete remains wet, some salts may penetrate into the concrete from the surface by diffusion. However, if the wetting period is short, the entry of salt water is mainly by absorption. The salts are carried into the interior of the concrete and further concentrated during the next drying cycle. Below the outer convection zone of the cover, the concrete remains moist and chlorides penetrate further by

diffusion regardless of the external moisture conditions (Hong and Hooton, 1999, Hunkeler, 2005).

Cyclic wetting and drying can increase the rate of corrosion in reinforced concrete structures as a result of two actions. First, cyclic wetting and drying concentrates ions, such as chlorides, and can increase the rate of corrosion by the evaporation of water during the drying phase, allowing oxygen ingress. Secondly, once chloride thresholds have been reached at the depth of the steel, drying of the concrete increases the availability of oxygen required for steel corrosion, because oxygen has a substantially lower diffusion coefficient in saturated concrete (Hong and Hooton, 1999). Concrete structures subjected to cyclic wetting and drying by seawater (tidal zone) are therefore more prone to deterioration than those permanently submerged (submerged zone) (Abdul-Hamid *et al*., 1990).

2.4.1.8 ***Effect of sustained loading and loading history on corrosion rate***

Cracks increase in number, width and depth under the effect of sustained and/or cyclic loading. Cracks that are generated by sustained loads or overloads, or both, may influence the corrosion response of the reinforcing steel. The growth rate of cracks is considerably faster, and hence concrete may deteriorate more rapidly, under cyclic loading than under sustained loading (Ahn and Reddy 2001). It has been observed that, under sustained loading, cracks grow in width but at a decreasing rate (ACI-224, 2001).

Yoon *et al*. (2000) studied the influence of pre-loading (or pre-cracking) and sustained loading on corrosion propagation using 100 x 150 x 1170 mm beam specimens made with w/b ratio of 0.5 and a concrete cover of 30 mm. The pre-loaded specimens were loaded to 45% and 75% of the ultimate flexural load and then unloaded, while the specimens under sustained loading were loaded to 20, 45, 60 and 75% of the ultimate flexural load and the load sustained on the specimens during the corrosion tests. The respective load levels were maintained by checking beam deflections using linear variable displacement transducers (LVDTs). The specimens were subjected to a cycle of 4 days wetting and 3 days drying with 3% NaCl solution. The following conclusions were made:

- For both the sustained load and pre-loaded specimens, corrosion rate was higher in the specimens loaded to higher load levels e.g. specimens loaded to 75% of the ultimate flexural load had apparently roughly higher corrosion rates (measured in terms of steel mass loss) than those loaded to 45% of the ultimate flexural load (Figure 2.14)
- For the same loading level, specimens under sustained loading had higher corrosion rates than the pre-cracked ones (Figure 2.14).

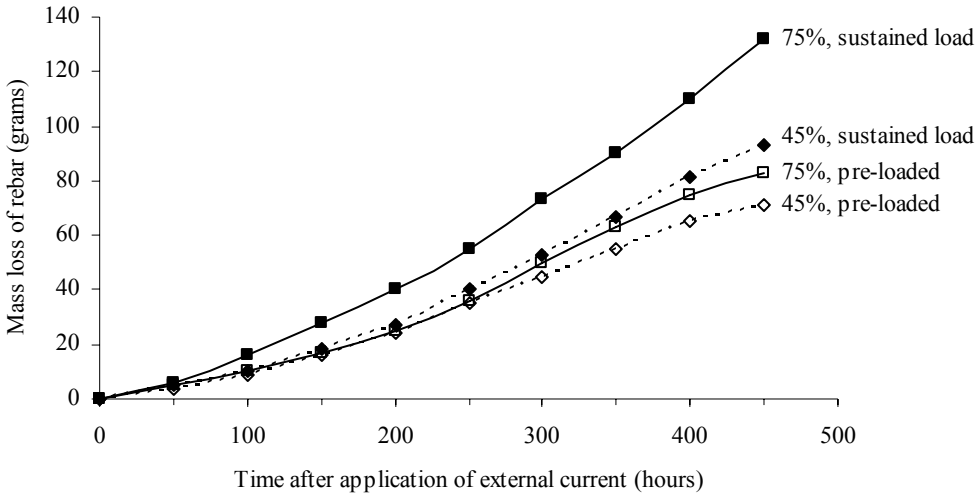

Figure 2.14: Effect of pre-loading and sustained loading on corrosion propagation (Yoon *et al*., 2000)

The high corrosion rates in the specimens under sustained loading and those at higher loading levels was attributed to increased number, size and interconnectivity of cracks which increase the penetrability of the concrete. The low corrosion rates in the pre-loaded specimens was attributed to cracks being closed or becoming smaller and less connected after unloading thus slowing down penetration of corrosion agents (chlorides and oxygen) and thus reducing corrosion rate. Crack self sealing may also be an explanation to the low corrosion rates in the pre-loaded specimens but this was not explored in this study.

It can therefore be concluded that both the loading history and loading level play important roles in corrosion propagation.

2.4.1.9 ***Influence of concrete resistivity***

Electrical resistivity is an important physico-chemical property of concrete that affects a variety of its applications. It is the ratio between applied voltage and resulting current. It is a geometry-independent material property which describes the electrical resistance of a material (Rilem TC 154-EMC, 2000). It is related to the penetrability of fluids and diffusivity of ions through porous materials such as concrete (Marta and Jezierski, 2005). Over recent years, concrete electrical resistivity is increasingly being used to indirectly evaluate concrete characteristics such as chloride ion diffusivity and degree of saturation. It can also be used to provide useful information on reinforcement corrosion of concrete (Morris *et al*., 1996).

Electrical resistivity (or its inverse, conductivity) is a measure of the ability of concrete to resist the passage of electrical current. It is an important component of corrosion cells, as high resistivity of the electrolyte (in this case concrete pore solution) and the physical pore structure (such as interconnectivity and tortousity) will reduce corrosion currents and slow the

rate of corrosion. It is related to both pore structure and the chemistry of pore solution (Shi, 2004).

In spite of the studies done on concrete resistivity, it is not yet possible to accurately predict the resistivity of a given concrete from knowledge of the respective constituents and mixture proportions alone. This is because the resistivity of concrete is affected by both concrete intrinsic and extrinsic factors.

Electrical resistivity can be used as an indirect measure of the probability of corrosion initiation and its propagation. A resistivity of less than 5 kΩ-cm can support very rapid corrosion of steel (Brown, 1980). If the electrolyte has high resistance to the passage of current, or if the concrete is dry and unable to support ionic flow, then corrosion will occur only at a very low rate. Various researchers have concluded that corrosion can be limited by increasing concrete resistivity (Tremper, 1958, Vassie, 1980, Alonso *et al*., 1988, Scott, 2004).

The electrical resistivity of concrete may vary over a wide range, from 1 to 10^4 kΩ-cm. It is influenced by many factors including the binder type and content, w/b ratio, degree of pore saturation, type of aggregate, presence of salts such as chlorides, temperature and age of the concrete (Gjorv *et al*., 1977).

There are no generally accepted rules relating resistivity to corrosion rate. The relationship between concrete resistivity and corrosion rate is still a subject under study. However, a commonly used guide has been suggested for the interpretation of measurements of the likelihood of significant corrosion for non-saturated concrete as presented in Table 2.12 (Andrade and Alonso, 1996).

Table 2.12: Relationship between resistivity and corrosion risk (Andrade and Alonso, 1996)

Resistivity (kΩ-cm)	*Risk level*
> 100 - 200	Very low Corrosion rate even if chloride contaminated
50 - 100	Low corrosion rate
10 - 50	Moderate to high corrosion rate
< 10	Resistivity is not the controlling parameter

Further, the corrosion current density has been shown to be inversely proportional to the resistivity of concrete or directly proportional to its conductivity (Hunkeler, 2005):

$$i_{corr} \approx \frac{1}{R_c} = \sigma_c \qquad (2.14)$$

where: i_{corr} = corrosion current density (A/cm^2)
R_c = concrete resistivity (Ω)
σ_c = concrete conductivity

However, this is subject to a number of factors such as cover to reinforcement, degree of concrete saturation, presence of cracks, presence of salt ions, w/b ratio etc. Therefore, resistivity must be analysed in conjunction with other corrosion influencing factors.

2.4.2 ***Prediction of corrosion propagation period***

The propagation period (t_p) defines the time necessary for sufficient corrosion to occur and cause unacceptable level of damage to the RC structure or element. The length of this period depends on the definition of *unacceptable damage* or an *acceptable limit state*. This level of damage will vary depending on the requirements of the owner and the nature or use of the structure. For example, ACI committee 365 (2005) defines the propagation period as the *time to first repair*.

Consequently, the length of the propagation period depends principally on the corrosion rate, which in most cases is related to loss of steel cross sectional area, time to cracking, and gradual loss of steel/concrete bond (Andrade and Alonso, 1996). However, most service life prediction models do no explicitly account for these effects. The following sections will cover briefly some of the criteria used to predict the duration of the corrosion propagation period.

2.4.2.1 ***Prediction based on loss of steel cross-sectional area***

The design of a structure is governed by the various national codes which stipulate design and construction from one country to another, but there is generally quite a large safety factor built into the calculations to accommodate variations in material properties, construction and loading. These safety factors can effectively accommodate a certain loss in cross sectional area which may be used to define the *acceptable damage*. Andrade and Alonso (1996) suggest a loss of cross sectional area between 5% and 25% to define the end of service life of the structure. This range seems to be a reasonable estimate for the end of a structure's service life, taking into account the in-built safety factors already mentioned.

The relationship between corrosion rate and loss of cross section is based on Faraday's Law (Stansbury and Buchanan, 2000):

$$m = \frac{MIt}{zF} \tag{2.15}$$

where: m = mass of metal entering solution (g)

M = atomic mass (g/mol)

I = corrosion current (A)

t = time (seconds)

z = valency of metal

F = Faraday's constant (96,500 C/mol)

2.4.2.2 ***Prediction based on time to corrosion-induced cracking***

Corrosion cracks, unlike service cracks, run longitudinal with the steel and may allow for a significant acceleration of the corrosion rate as the steel is more directly exposed to the atmosphere and the ability of the cement extenders to provide protection is reduced. Thus the onset of corrosion-induced cracking may also provide a reasonable, though conservative, estimate to the end of a structure's life and can therefore be used to estimate the propagation period (Liu and Weyers, 1998).

Several models have been developed to predict the time to cracking, for example Bazant's physical-mathematical model (1979), Cady and Weyers' model (1983), Morinaga's empirical model (1990), Liu and Weyers' mathematical model (1998) and El Maaddawy and Soudki's mathematical model (2006)). Liu and Weyers' (1998) mathematical model is presented here as an example. It is related to the critical mass of corrosion products and corrosion rate and is given by the equation:

$$T_{cr} = \frac{W_{crit}^2}{2k_p} \tag{2.16}$$

where: T_{cr} = time to cracking (years)

W_{crit} = critical volume of rust products required to induce cracking

k_p = $0.098(1/\alpha)\pi D i_{corr}$

D = diameter of reinforcing

α = 0.57, mean of corrosion products $Fe(OH)_2$ and $Fe(OH)_3$ where α is equal to 0.523 and 0.622 respectively

i_{corr} = annual mean corrosion current density (mA/ft^2)

A detailed description of the model and its development can be found in Liu and Weyers (1998). The other time-to-cracking models mentioned can be found in the respective references.

The next chapter will cover the various methods that can be used to assess corrosion, with a focus on chloride-induced corrosion.

3 MEASUREMENT OF CORROSION

3.1 ***Introduction***

The evaluation of the condition of corroding RC structures is normally a two-stage process involving preliminary and detailed measurements. The preliminary assessment characterises the nature of the corrosion and gives guidance in planning detailed measurements. It involves a visual inspection such as probing of cracks and spalls to see their extent. The detailed assessment will then confirm the cause and quantify the extent of corrosion. This stage will show the extent of damage that has occurred and the cause(s) of the damage. Table 3.1 lists some of the techniques that can be used for corrosion assessment and what they detect.

Table 3.1: Corrosion assessment techniques (Heckroodt, 2002)

Classification	*Assessment*	*Detects*
Preliminary	• Visual inspection • Half-cell potential • Resistivity measurements	• Surface defects such as rust stains, spalling • Probability of corrosion (Electrochemical state of the steel) • Probability of corrosion
Detailed	• Carbonation depth • Chloride content • Linear polarization	• Carbonation ingress • Chloride ingress • Corrosion rate

3.2 ***Visual inspection***

Visual inspection is usually the first step in an investigation. The aim is to give a first indication of what is wrong and how extensive the corrosion damage is. For example, if the concrete is spalling, this can be used as a measure of extent of damage. However, visual inspection can only provide useful information when done in a rational and systematic manner. Classification of visual evidence of deterioration must be done objectively, following clear guidelines that define damage in terms of appearance, location and cause. Defects may be defined in terms of (Heckroodt, 2002):

- Cracks: caused by corrosion, temperature gradient loading, shrinkage or fatigue
- Joint deficiencies: joint spalls, upward movement, lateral movement, seal damage
- Surface damage: abrasion, rust stains, delaminations, popouts, spalls
- Changes in member shape: curling, deflection, settlement, deformation
- Textural features: blow holes, honeycombing, sand pockets, segregation

The accuracy of interpretation of the results of a visual inspection is mainly based on the experience of the person conducting the survey. Visual surveys should be followed up by testing to confirm the cause of corrosion (Rodriguez *et al*., 1994). It must also be noted that corrosion-induced structural deterioration is a gradual process with a commencement time not always obvious from external examination (Li *et al.*, 2008).

Visual inspection therefore only serves as an indication of an already ongoing corrosion process in the concrete. Moreover, it may come too late for cost-effective repairs because reinforcement corrosion damage only manifests itself at the surface after significant deterioration has occurred.

A visual inspection should include the parameters listed in Table 3.2.

Table 3.2: Visual inspection (Heckroodt, 2002)

Feature	*Description*	*Cause*	*Details*
Cracking	Jagged separation of concrete, cracking along reinforcement pattern	Overload, corrosion, shrinkage, thermal gradient, chemical deterioration e.g. ASR	Direction, width, depth, pattern
Rust stains	Brown stains on concrete surface	Corrosion of steel, tying wire or surface steel work	Area
Spalling	A fragment of concrete detached from a larger mass	Exertion of internal pressure due to rebar corrosion or external force	Area, depth

3.3 Half-cell potential measurement

This is an electrochemical method (also referred to as *open circuit* or *corrosion potential*) and is currently one of the most widely used methods for the detection of the potential for steel reinforcement corrosion in concrete. The principle of this method is based on the measurement of the potential difference between the reinforcement and a reference electrode in the form of a half-cell (Rodriguez *et al.*, 1994, Broomfield *et al*., 2002). The technique is particularly useful because it can be utilized to evaluate the probability of corrosion before damage is evident at the surface of a RC structure.

The half-cell is a simple device consisting of an electrode and an electrolyte. The electrolyte is normally made from a soluble salt of the electrode metal i.e. the reference electrode is a piece of metal in a solution of its own ions, such as copper/copper sulphate ($Cu/CuSO_4$), Calomel (Hg/Hg_2C1_2) and silver/silver chloride (Ag/AgCl).

Half-cell potential (E_{corr}) measurement is based on the electrical and electrolytic continuity between the embedded steel, reference electrode on the concrete surface and the voltmeter. A high impedance digital voltmeter is used to collect the data, connecting the electrode and the reinforcement as shown in Figure 3.1. The voltmeter should have high input impedance so that the current flowing through the reference electrode does not disturb the stability of the reference electrode potential. Electrical conduction between the reference electrode and the concrete is established by the transport of ions. In practice, this can be ensured by placing a wet sponge between the reference electrode and the concrete surface.

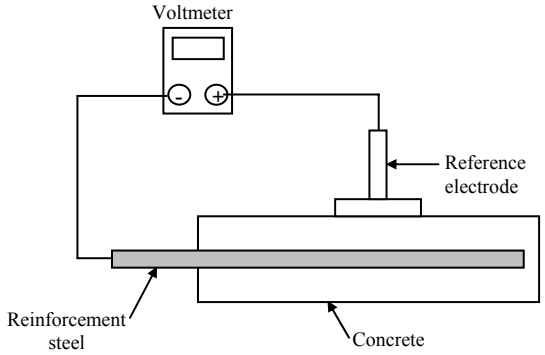

Figure 3.1: Schematic of half-cell potential measurement (Broomfield *et al*., 2002)

The numerical value of the measured potential between the embedded steel and the reference electrode will depend on the type of reference electrode used and the corrosion condition of the steel in the concrete. It is therefore important to quote the reference electrode being used for half-cell potential measurements. For site work, saturated $Cu/CuSO_4$ electrode is most robust and is sufficiently accurate, although errors may arise due to contamination of the concrete surface with copper sulphate. Calomel and silver chloride electrodes are used more in laboratory work due to their stability and robustness. The base potential of the reference electrodes depends on the concentration of the electrolyte and therefore care has to be taken to maintain the electrodes in saturated conditions.

Half-cell potential measurements can be used for the following applications:

(i) Detection of corroding steel bars; the criteria for corrosion are illustrated in Table 3.3. It is important to note that HCP measurements only give an indication of the corrosion risk of steel and are linked empirically to the probability of corrosion.

(ii) Defining positions for additional tests (such as corrosion current measurement, chloride profiles and embedding of sensor for monitoring).

(iii) Design of cathode and anode layout for cathodic protection or electrochemical repair

(iv) Assessment of corrosion state in concrete after repair

(v) Potential mapping: Half-cell potential values can be plotted and contours of equal potential drawn through the points of equal or interpolated values (Vienna, 2002). This result is an equipotential contour map (Figure 3.2).

Table 3.3: Criteria for corrosion of steel in concrete (ASTM C876-91, 1999)

Cu/CuSO$_4$ electrode	*Ag/AgCl electrode*	*Likely corrosion condition*
> -200 mV	> -106 mV	Low (10% risk of corrosion)
-200 to -350 mV	-106 to -256 mV	Intermediate corrosion risk
< -350 mV	< -256 mV	High (>90% risk of corrosion)
< - 500 mV	< - 406 mV	Severe corrosion

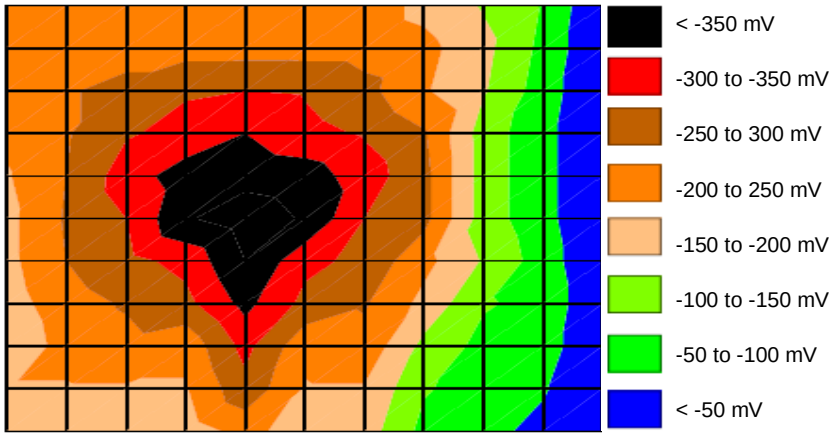

Figure 3.2: Equipotential contour map showing variation of potentials within a concrete sample (Vienna, 2002)

Half-cell potential measurements are affected by various factors which should be considered during their interpretation. Some of these are briefly discussed:

(i) *Oxygen concentration*: Oxygen concentration at the concrete-steel interface may affect the half-cell potential readings significantly. A decrease in oxygen concentration at the surface of the steel will result in a more negative corrosion potential reading. This kind of negative potential reading may not necessarily be associated with a high probability of steel corrosion. For example, steel reinforcement underneath a dense concrete cover with low permeability would have more negative corrosion potential readings than a porous concrete with a higher permeability but such negative readings do not necessarily indicate a high probability of corrosion (Elsener and Bohni, 1997, Frølund *et al*., 2003).

(ii) *Concrete resistivity*: A high concrete resistance can introduce significant errors in the half-cell potential measurements. Figure 3.3 is a schematic diagram illustrating a half-cell potential measurement circuit. The measured half-cell potential reading is the potential between the two ends of the voltmeter internal resistor. It is only when this

resistance is much larger than the concrete resistance that the measured half-cell potential reading is close to the true corrosion potential of the steel reinforcement. There are ways to increase the accuracy of the measurement (Andrade *et al*., 2003):

- Decreasing the concrete resistance e.g. by wetting the concrete surface
- Using a voltmeter with a high internal resistance
- Positioning the reference electrode on the concrete surface directly above the steel reinforcement. This can also decrease the concrete resistance and increase the measurement precision.

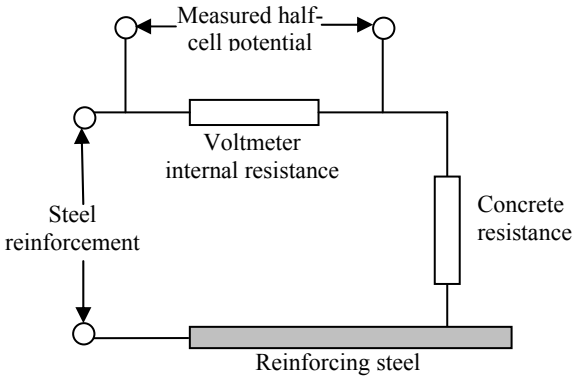

Figure 3.3: Schematic illustration of half cell potential measurement circuit (Andrade *et al*., 2003)

3.4 ***Concrete resistivity measurement as a corrosion assessment criteria***

Resistivity measurement of concrete is mainly used as an indicator of reinforcement corrosion activity and its potential severity (Broomfield, 1997, Gowers and Millard, 1999). The relationship between concrete resistivity and corrosion rate was covered in section 2.4.1.9 and will therefore not be reviewed here again. Concrete resistivity measurement techniques will be briefly covered in this section.

3.4.1 ***Single electrode resistivity measurement technique***

This method is based on using a small metallic contact disc placed on the concrete surface as an electrode and a reinforcing steel bar as a counter-electrode as shown in Figure 3.4 (Feliu *et al*., 1996, Broomfield, 1997). It requires a connection to the reinforcement cage and full steel continuity (Rilem TC 154-EMC, 2000).

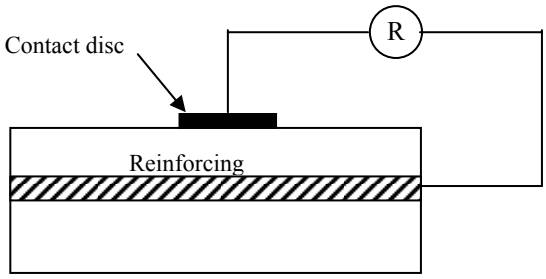

Figure 3.4: Set-up of one electrode (disc) resistivity measurement of concrete (Rilem TC 154-EMC, 2000)

Concrete resistivity (ρ) is calculated using the following equation (Broomfield, 1997):

$$\rho = 2RD \ (k\Omega\text{-}cm) \tag{3.1}$$

where D is the diameter of the metallic disc (*cm*) and R its resistance ($k\Omega$).

3.4.2 ***Two-probe resistivity measurement technique***

This method is based on passing an alternating current between two electrodes placed on a concrete surface and measuring the potential between them (Figure 3.5). It is a very simple technique but has significant limitations and sources of error.

One main disadvantage is that the measurement is influenced by the area of concrete in close proximity to the electrode tip (Millard, 1991). If the electrode is placed directly over a piece of aggregate, the reading may be much higher than the actual concrete resistivity. This is because aggregate resistivity is generally much higher than that of the surrounding matrix.

The contact radius has a significant effect on resistivity measurement using this method. A smaller contact radius will cause a higher resistivity reading than that obtained with a large radius over a given area of concrete. Millard (1991) indicated that 90% of the resistivity reading represents an area with a diameter equivalent to 10 times the contact radius of the electrode tip.

A common but not practical procedure to reduce errors associated with this method is to place the electrodes in pre-drilled holes filled with a conductive medium in order to provide good contact with the concrete (Gowers and Millard, 1999).

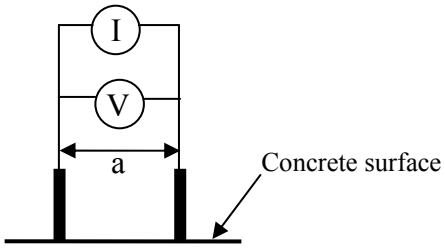

Figure 3.5: Schematic drawing of two-probe resistivity meter
(Gowers and Millard, 1999)

*3.4.3 **Four-probe (Wenner) resistivity measurement technique***

The four-probe (Wenner) method is currently the most widely used technique for measurement of concrete resistivity. The apparatus consists of four electrodes equally spaced (Figure 3.6). A small current of low frequency is applied between the outer probes and potential drop measured between the inner probes (Millard *et al*., 1990).

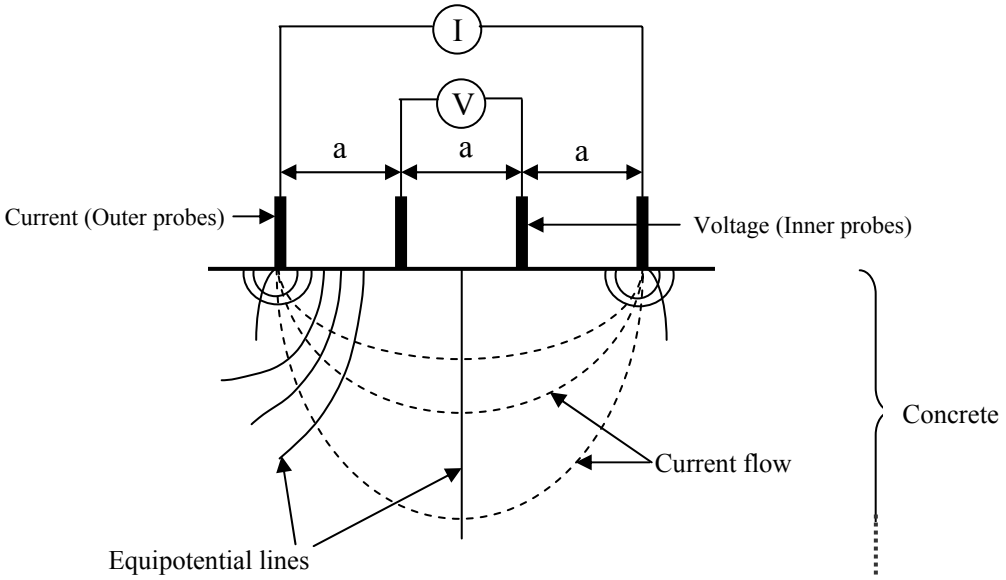

Figure 3.6: Schematic drawing of four-probe (Wenner) method resistivity measurement
(Vienna, 2002)

The apparent resistivity (ρ) in Ω-cm may be expressed as:

$$\rho = \frac{2\pi a V}{I} \qquad (3.2)$$

where V = voltage drop, Volts

I = applied current, amperes

a = electrode spacing, cm

This calculation assumes the concrete to be homogeneous, and the non-homogeneity caused by the reinforcement network should be minimised by using an electromagnetic cover meter or bar detector to determine the position of steel reinforcement.

One advantage of this technique over the two-probe arrangement is that it measures the resistivity of the concrete area between the inner probes which is a larger area than that of the probe tip. The influence of aggregate can therefore be avoided when the spacing between the inner electrodes exceeds the maximum size of the aggregate particles. This will yield a more reliable resistivity reading. A spacing of 50 mm is sufficient to give relatively accurate resistivity readings for most concrete structures (Millard, 1991).

There are several factors which influence the resistivity measurement when the four-probe technique is used (Whiting and Nagi, 2003) including:

(i) geometrical constraints
(ii) surface contact
(iii) concrete non-homogeneity
(iv) presence of steel reinforcing bars
(v) surface layers having different resistivity than the bulk of the concrete and
(vi) ambient environmental conditions

Gowers and Millard (1999) investigated these factors, and the findings are summarized below:

- The size of the concrete structure compared to the electrode spacing has an effect on resistivity measurements. Wenner four-probe method is based on the assumption that resistivity values are accurate if current and potential fields exist in a semi-infinite volume of material. Therefore, resistivity readings will be more accurate for structures with relatively large dimensions.
- Significant errors occur in measuring thin concrete members or near edges. It is recommended that the spacing between electrodes not exceed ¼ of the minimum concrete section dimension.
- Surface contacts are less critical for the four-probe method than for the two-probe technique. However, adequate electrical contact should be established between electrodes and the concrete surface, such as by use of a conductive gel. An uneven electrical contact between these contacts and the surface of the concrete can lead to significant errors. The use of a relatively low frequency alternating current applied current, approximating to direct current, helps to minimize this effect.
- Inhomogeneities affect electrical resistivity measurements using the Wenner method. However, it is assumed that the concrete is homogenous. For example a high-resistivity aggregate surrounded by low-resistivity cement paste is a source of such inhomogeneities.

This can be reduced by increasing the spacing between the inner electrodes. It was found that the coefficient of variation in resistivity measurements will not exceed 5% if the spacing between the inner electrodes is greater than 1.5 times the maximum aggregate particle size.

- The presence of steel is an important factor influencing the electrical resistivity of reinforced concrete. Gowers and Millard (1999) showed that the errors associated with the presence of steel are significant only when measurements are taken directly over a reinforcing bar. Errors can be minimized if measurement is taken between bars or orthogonal to a bar.
- The difference in resistivity between the surface layer and the underlying concrete will have an influence on field resistivity measurements. If the resistivity of the surface layer is higher than that of the underlying concrete, such as in the case of a carbonated surface, the error in measured resistivity of the underlying concrete will be small. However, if the surface layer resistivity is low, such as might be caused by the ingress of chlorides into the concrete surface layer, the error in measured resistivity of the underlying concrete will be more significant. While the presence of a single surface layer can easily cause significant errors in the resistivity measurement of the underlying concrete, a double surface layer can cause quite inconsistent results that may not be so easily minimized or compensated (Gowers and Millard, 1999).

3.5 Chloride content measurement

Total chloride content in the concrete is usually measured by a titration process that involves dissolving concrete powder samples in acid. Samples are taken from in-situ drilled concrete cores or powder concrete samples. The samples are taken at different depths so that the chloride profile (i.e. the variation of chloride concentration with depth) and the variation of total chloride content (by mass of binder) with depth into the concrete can be determined.

The chloride content at the rebar level determines the likelihood of corrosion depending on the critical chloride content, but the profile can be used to predict the future rate using Fick's second law of diffusion (see section 2.3.5.2).

3.6 Linear polarization resistance (LPR) measurement

The theory of linear polarization, also known as polarisation resistance, relies on the relationship between the half-cell potential of a piece of corroding steel and an external current applied to it i.e. the reinforcing steel is perturbed by a small amount of potential from its equilibrium potential.

Three electrodes are used viz counter/auxilliary, working, and reference electrodes. The counter electrode applies current or potential to the embedded steel reinforcement, which is the working electrode. The reference electrode (e.g. Ag/AgCl) measures the change in potential due to applied current or potential.

A schematic of the linear polarization set-up is shown in Figure 3.7. It has a control box (pulse generator) that applies the current or potential, a multimeter and a data logger that records the measurement, a half cell to measure the potential and its change, and a counter electrode to pass the applied current/potential to the working electrode (corroding reinforcement) (Flis *et al*., 1993, Broomfield, 1997).

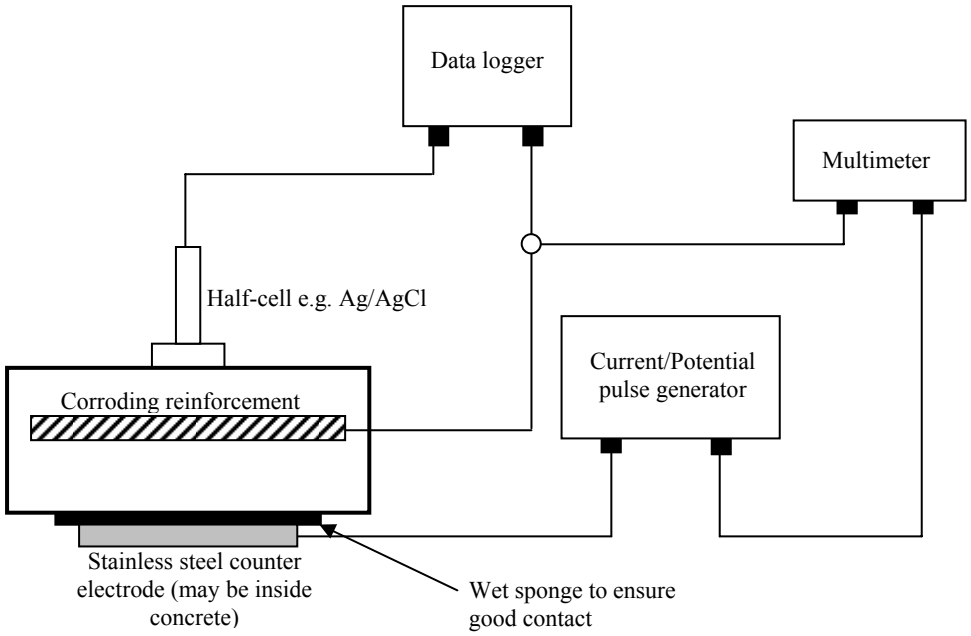

Figure 3.7: Schematic of polarisation resistance measurement device (Richardson, 2002)

Measurements are performed by applying a potential either as a constant pulse (potentiostatic), or a potential sweep (potentiodynamic), and measuring the current response. Alternatively, a current pulse (galvanostatic) or a current sweep (galvanodynamic) can be applied, and the potential response measured.

In each case, the conditions are selected such that the ΔE falls within the linear Stern-Geary range of ±10 to 20 mV (Figure 3.8). When a very small electrical potential (of the order of 10 mV) is applied to the corroding steel, the relationship between potential and current is linear. As shown in Figure 3.8 there is an approximately linear position in the region of the open circuit/half-cell potential. The linear polarization device (Figure 3.7) applies a small electrical current ΔI (or ΔE) and measures the shift in potential, ΔE. The ratio of the applied potential to

resulting current ($\Delta E/\Delta I$) is called the polarization resistance (R_p) and is inversely proportional to the corrosion current, I_{corr}, (Stern and Geary, 1957).

$$I_{corr} = \frac{B}{R_p} \tag{3.3}$$

where: R_p = change in potential (ΔE)/change in current (ΔI)

B = a constant parameter (Stern-Geary constant) varying from 26 to 52mV depending on the passive (52 mV) or active (26 mV) condition of the steel.

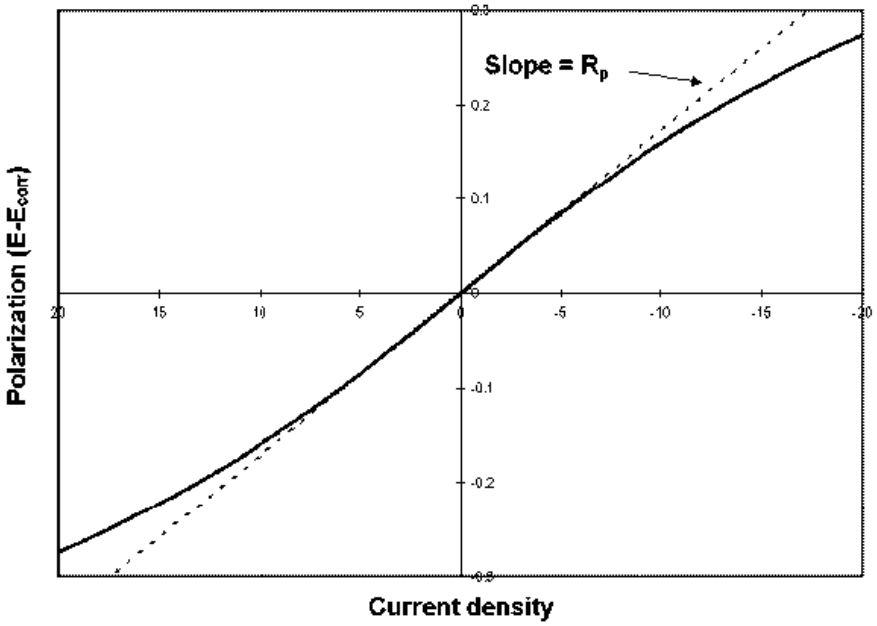

Figure 3.8: Linear polarisation curve (Stern and Geary, 1957)

In order to calculate a corrosion rate with the LPR technique, the following fundamental assumptions are made (Hansson *et al*., 2007):

- uniform corrosion damage
- there is a single anodic and a single cathodic reaction
- the proportionality constant between corrosion rate and R_p (i.e. B) must be known
- the electrical resistance of the solution (i.e. the concrete pore solution) is negligible
- the half-cell potential is stable

Of these assumptions, only the second one is applicable to the case of chloride-induced corrosion of embedded reinforcement.

The corrosion rate (in terms of current density per given steel surface area) can be deduced as follows:

$$\text{Corrosion rate } (i_{corr}) = \frac{I_{corr}}{A} \ (\mu A/cm^2) \qquad (3.4)$$

Where A is the polarized steel surface area (A=ЛDl cm^2 where D is the diameter of the steel and l is the length of the polarized steel area).

The major limitation of this technique is difficulty in knowing the actual surface area of steel that is polarized by the applied potential, or the area which is actively corroding. Therefore, the corrosion is generally considered to be uniform over the polarized area and the measured corrosion current is divided by the estimated polarized area to give an average corrosion rate.

An additional limitation is that this is an instantaneous corrosion rate and neither (*a*) gives an indication of how long corrosion has been going on nor (*b*) how the corrosion rate varies with time and ambient conditions. A fundamental drawback of these measurements is that artificial corrosion damage and rebar surface changes can be induced at relatively high polarization levels.

Despite this, the LPR technique is popular for measuring corrosion rate because: (*i*) it is a non-destructive technique; (*ii*) it is simple to apply and (*iii*) it usually needs only a few minutes for corrosion rate determination.

Classification of measured corrosion rates as proposed by Rodriugiez *et al.,* (1994) is given in Table 3.4.

Table 3.4: Interpretation of measurements (Rodriugiez *et al.,* 1994)

Current density (μA/cm^2)	*Corrosion state*
< 0.1 - 0.2	Passive condition
0.2 - 0.5	Low to moderate
0.5 - 1.0	Moderate to high
> 1.0	High

To overcome the problem of accurate determination of the actual area of steel polarised (especially for on-site applicaiton), commercial LPR devices such as GECOR-6 and GECOR-8 make use of a guard ring around the counter/auxilliary electrode to constrain the applied electric field from the counter electrode. This ensures that a measurement is taken from a defined area of steel and prevents gross errors in the estimation of area of steel (Figure 3.9).

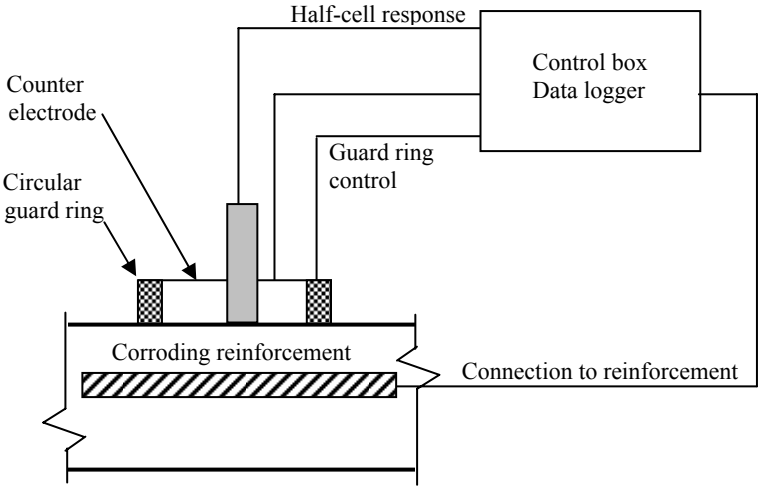

Figure 3.9: Schematic of polarisation resistance measurement with a guard-ring incorporated (Modified from Richardson, 2002)

3.6.1 ***Coulostatic technique***

The coulostatic technique is essentially a galvanostatic LPR technique which measures the relaxation of the potential after a small fixed current (ΔI) is applied to the reinforcing steel for a known duration in the order of milliseconds. Corrosion rates are related to a time constant describing the potential decay (ΔE) induced by a small charge (10-20 mV) disturbance.

A high corrosion current will lead to a rapid decay of the potential transient whereas with a lower corrosion current the decay of the potential after the perturbation will take a longer time. The potential transient is described by the equation (Glass, 1995, Hassanein *et al*., 1998):

$$n_t = n_o \exp\left(\frac{-t}{\tau_c}\right) \tag{3.5}$$

where n_t = potential shift at time t

n_o = initial potential shift

τ_c = time constant

The polarization resistance R_p is then obtained from the time constant and capacitance (C) information, with q_s being the applied charge density.

$$\tau_c = CR_p \tag{3.6}$$

$$C = \frac{q_s}{n_o} \tag{3.7}$$

Potential measurements are taken 0.1 seconds after the termination of the charge which allows many of the very earlier transients to dissipate. The remaining early additional transients are

unlikely to significantly effect the corrosion rate measurements as potential readings are taken for at least 30 seconds thus the overall shape of the curve and the resulting equation are still valid.

The duration of the charge has been shown by Glass (1995) to have an effect on the shape of the relaxation transient with longer perturbations resulting in progressively flatter relaxation curves as seen in Figure 3.10, resulting in underestimation of polarisation resistance (R_p) which then translates to overestimation of the actual corrosion rate. The flatter relaxation curves may be caused by an effective shift in time zero leading to the loss of the fast components of the transient related to the charging process as well as significant mass transfer occurring during the perturbation period which then affects the subsequent decay.

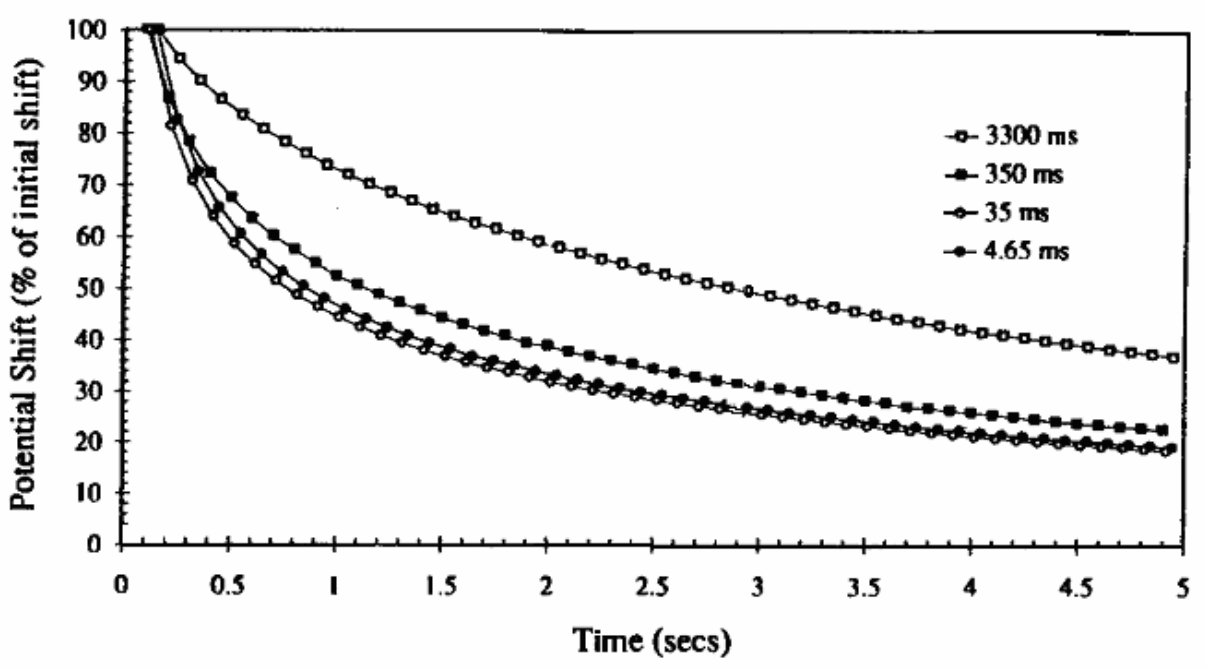

Figure 3.10: Effect of perturbation duration on shape of potential transients (Glass 1995)

The advantages of the coulostatic method include:

(i) A very small perturbation is applied during which the effects of diffusion can be minimised by keeping the perturbation period short
(ii) No need to compensate the result for the effects of the electrolyte
(iii) The determination of the interfacial capacitance as part of the measurement
(iv) Its suitability for low frequency work when compared with impedance measurements
(v) The insensitivity of the time constant to the steel surface area

The disadvantages include:

(i) The long time required to determine the transient compared to direct polarisation resistance measurements particularly for passive steel and

(ii) The need for independent verification of the accuracy of the method
(iii) Determination of the actual area of the embedded steel that is corroding
(iv) It neither gives an indication of how long corrosion has been going on nor how the corrosion rate varies with time and ambient conditions.

However, coulostatic methods provide additional information on the corroding interface which may lead to an improved understanding of the processes occurring.

*3.6.2 **Cyclic potentiodynamic polarization***

This is a non-destructive technique that provides information on the corrosion rate, corrosion potential and susceptibility to pitting corrosion of the metal in the test environment (in this case concrete), as well as information about the expected behavior of the steel should its potential be changed by, for example, exposure to stray currents, coupling with other metals, or when the surrounding concrete becoming anaerobic (Hansson *et al*., 2007).

In this method, the potential of the specimen is changed continuously or in steps, while the resulting current is monitored. Like most electrochemical techniques, cyclic polarization is carried out with three electrodes viz, a working electrode (the reinforcing steel), a counter electrode and a reference electrode.

Cyclic polarization is most useful in the laboratory but has the same limitation of LPR of not knowing the actual polarized area of the steel, as well as taking a longer time to perform. It is the test method adopted in the ASTM standard G61-86 (2003).

REFERENCES

ACI Committee 201 (ACI 20R-92), (1992), Guide for making a condition survey of concrete in service, *American Concrete Institute*, Detroit, MI, pp. 30.

ACI Committee 222, (1996), Corrosion of metals in concrete, ACI 222R-96, *American Concrete Institute*, Detroit, MI, pp. 30.

ACI Committee 223R-95, (1995), Ground granulated blast furnace as a cementitious constituent in concrete, ACI 223R-95, *American Concrete Institute*.

ACI Committee 224R-01, (2001) - Control of cracking in concrete structures, *American Concrete Institute*.

ACI Committee 318 (ACI 318-89), (1992), Building code requirements for reinforced concrete, *American Concrete Institute*, Detroit.

ACI Committee 357 (ACI 357-R), (1997), Guide for the design and construction of fixed offshore concrete structures, *American Concrete Institute*.

Ahn, W. and Reddy, D.V., (2001), Galvanostatic testing for the durability of marine concrete under fatigue loading, *Cement and Concrete Research*, 31, pp. 343-349.

AASHTO T260-97, (1997), Standard method of test for sampling and testing for chloride ion in concrete and concrete raw materials, *American Association of State Highway and Transportation Officials*, Washington, D.C.

Aldea, C. M., Shah, S. P. and Karr, A., (1999), Permeability of cracked concrete, *Materials and Structures*, (32), June, pp. 370-376.

Alexander, M. G. and Mackechnie, J. R., (2002), A pragmatic prediction model for chloride ingress into concrete, presented at *RILEM Workshop*, Madrid, September 2002.

Alexander, M. G. and Mindess, S., (2005), *Aggregates in Concrete*, published by Taylor and Francis.

Alexander, M. G. and Beushausen, H., (2007), Performance-based durability design and specification in South Africa, *proceedings of International Concrete Conference and Exhibition* (ICCX – Concrete Awareness), 14-16 February 2007, Cape Town, South Africa, pp. 12-15.

Alonso, C., Castellote, M., Andrade, C., (2002), Chloride threshold dependence of pitting potential of reinforcements, *Electrochimica Acta* ,47, pp. 3469-3481.

Alonso, C., Andrade, C., Castellote, M. and Castro, P., (2000), Chloride threshold values to depassivate reinforcing bars embedded in a standardized OPC mortar, *Cement and Concrete Research*, 30(7), pp. 1047-1055.

Andrade, C. and Page, C. L., (1986), Pore solution chemistry and corrosion in hydrated cement systems containing chloride salts: A study of cation specific effects, *British Corrosion Journal*, 21(1), pp. 49-53.

Andrade, C., (1993), Calculation of Chloride Diffusion Coefficients in Concrete from Ionic Migration Measurements, *Cement and Concrete Research*, 23(3), pp. 724-742.

Andrade, C., Gulikers, J., Polder, R. and Raupach, M., (2003), Half-cell potential measurements- Potential mapping on reinforced concrete structures, *Materials and Structures*, 36, pp 461-471.

Andrade, C., Rio, O., Castillo, A., Castellote, M. and d'Andrea, R., (2006), An NDT performance-related proposal based on electrical resistivity to the specification of concrete durability, *Proceedings of International RILEM Workshop on performance based evaluation and Indicators for concrete durability*, 19-21 March 2006, Madrid, Spain, pp. 51-58.

Andrade, C., Polder, R. and Besheer, M., (2007), Non-destructive methods to measure ion migration, Chapter five, *RILEM TC 189-NEC: State-of-the-art report*, Non-destructive evaluation of the penetrability and thickness of the cover, pp. 91-112.

Arya, C. and Ofori-Darko, F. K., (1996), Influence of crack frequency on reinforcement corrosion in concrete, *Cement and Concrete Research*, 26(3), pp. 333-353.

Arya, C. and Wood, L., (1995), The relevance of cracking in concrete to corrosion of reinforcement, *Concrete Society*, Technical report No. 44.

Arya, C. and Xu, Y., (1995), Effects of cement type on chloride binding and corrosion of steel in concrete, *Cement and Concrete Research*, 25(4), pp. 893-902.

Arya, C. and Buenfeld, N. R., (1987), Assessment of simple methods of determining the free chloride ion content of cement paste, *Cement and Concrete Research*, 17, pp. 907-918.

ASTM Special Technical publication 818, (1983), Corrosion of metals in association with concrete, ASTM.

ASTM C876-91, (1999) Standard test method for half-cell potentials of uncoated reinforcing steel in concrete, ASTM.

ASTM G61-86, (2003) Standard test method for conducting cyclic potentiodynamic polarisation measurements for localised corrosion susceptibility of Iron, Nickel- or Cobalt-based alloys.

ASTM D1411-04 Standard test methods for water-soluble chlorides present as admixtures in graded aggregate road mixes.

Bakker, R.F.M., (1983), Permeability of blended cement concretes, *Proceedings of the CANMET/ACI First International conference on the use of Fly ash, Silica fume, Slag and other mineral by-products in concrete*, pp. 589-605.

Basheer, *et al*., 2001, Assessment of the durability of concrete from its permeation properties – a review, *Construction and Building Materials*, 15, pp. 93-103.

Bazant, Z. P., (1979), Physical model for steel corrosion in concrete sea structures – application, *ASCE Structural Division Journal*, 105(6), pp. 1155-1166.

Beeby, A., (1983), Cracking, cover and corrosion of reinforcement, *Concrete International*, February, pp. 35-40.

Bentur, A., Diamond, S. and Berke, N., (1997), *Steel corrosion in concrete, Fundamentals and Civil Engineering Practice*, London: E & FN Spon, pp. 41-43.

Blundell, R., (1987), The effect of cementitious blast furnace slag on chloride permeability of concrete, Discussion on a paper by Rose J., Corrosion, concrete and restraints, *American Concrete Institute*, pp. 107-125.

Bockris, J., Conway, B., Yeager, E. and White, R. ed., (1981), Comprehensive treatise of electrochemistry, *Electrochemical Materials Science*, Vol. 4, Plenum Press: New York.

Boddy, A., Bentz, E., Thomas, M. D .A. and Hooton, R. D., (1999), An overview and sensitivity study of a multi-mechanistic chloride transport model, *Cement and Concrete Research*, (29), pp.827–837.

Breysse, D. and Gerard, B., (1997), Transport of fluids in cracked Media, *RILEM report 16* – Barriers to organic and contaminating liquids, ed. Reinhardt H. W., published by E & FN SPON, London, pp. 123-153.

Broomfield, J. P., Davies, K., Hladky, K., (2002), The use of permanent corrosion monitoring in new and existing reinforced concrete structures, *Cement & Concrete Composites*, (24), pp. 27–34.

Broomfield, J. P., (1997), *Corrosion of Steel in Concrete: Understanding, Investigation and Repair*, London, UK: E & FN Spon.

British Standards Institute BS 8110-1, (1997), *Structural use of concrete* - Part 1: Code of practice for design and construction.

British Standards Institute BS 5400-4, (1990), Code of practice for design of Concrete Bridges.

Buenfeld, N. R., Shurafa-Daoudi, M. T. S., and McLoughlin, I. M., (1997), Chloride transport due to wick action in concrete. In Nilsson L. O., and Olliver J. P., *Proceedings of RILEM international workshop on chloride penetration into concrete*, Paris: RILEM.

Cady, P. D. and Weyers, R.E., (1983), Chloride penetration and the deterioration of concrete bridge decks, *Cement, Concrete & Aggregate*, 5(2), pp. 81-87.

Castellote, M., Alonso, C., Andrade, C., Castro, P., and Echeverrõ, M., (2001), Alkaline leaching method for the determination of the chloride content in the aqueous phase of hardened cementitious materials, *Cement and Concrete Research*, 31, pp. 233-238.

Cervantes, V. and Roesler, J., (2007), Ground granulated blast furnace slag, *Technical note No. 35*, Dept. of Civil and Environmental Engineering, University of Illinois.

Cornell, R. and Schwertmann, U., (1996), *The Iron oxides*: Structure, Properties, Reactions, Occurrence and Uses, VCH, Weinheim.

Chrisp, T. M., McCarter, W. J., Starrs, G. , Basheer, P. A. M. and Blewett, J., (2002), Depth-related variation in conductivity to study cover-zone concrete during wetting and drying, Cement & Concrete Composites 24, pp. 415–426.

Daigle, L., Lounis, Z., Cusson, D., (2004), Numerical prediction of early-age cracking and corrosion in high performance concrete bridges – Case study; *Proceedings of Annual conference of the Transportation Association of Canada Innovations in Bridge Engineering*, Québec city, Québec.

DuraCrete, (1999), Models for environmental actions on concrete structures, *The European Union in Brite EuRam III*, pp. 273.

DuraCrete, (1998), Probabilistic performance based durability design: modelling of degradation, *DuraCrete project document*, BE95-1347/R4-5, The Netherlands.

Du Preez, A. A. and Alexander, M. G., (2004), A site study of durability indexes for concrete in marine conditions, Materials and Structures, 37, pp. 146-154.

Edvardsen, C., (1999), Water permeability and autogenous healing of crack in concrete, *ACI Materials Journal*, 96(4), pp. 448–454.

El Maaddawy, T. and Soudki, K., (2006), A model for prediction of time from corrosion initiation to corrosion cracking, *Cement & Concrete Composites*, 29(3), pp. 168-175.

Elsener, B. and Bohni, H., (1997), Half-cell potential measurements - From theory to condition assessment of RC structures, *Proceedings of International Conference on Understanding Corrosion Mechanisms of Metals in Concrete - A Key to improving Infrastructure Durability*, Massachusetts Institute of Technology, MIT (Cambridge, USA), 27-31 July 1997.

Elsener, B., (2001), Half-cell potential mapping to assess repair work on RC structures, *Construction Building Materials*, 15, pp. 133-139.

Elsener, B., Zimmermann, L. and Böhni, H., (2003), Non destructive determination of the free chloride content in cement based materials, *Materials and Corrosion*, 54, pp. 440-446.

Elsener, B., Andrade, C., Gulikers, J., Polder, R. and Raupach, M., (2003), Half-cell potential measurements- Potential mapping on reinforced concrete structures, *Materials and Structures*, 36, pp 461-471.

English, J., Fielding, M., Howard, E. and van der Merwe, N., (2006), *Professional Communication*: How to deliver effective written and spoken messages, 2nd Edition, published by Juta and Company Ltd, Landsdowne 7779, South Africa.

EN 206-1, (2000), Concrete Part 1: Specification, performance, production and conformity, *European Standards*.

Jana, D. and Erlin, B., (2007), Carbonation as an indicator of crack age, *Concrete International*, May, pp. 61-64.

Feliu, S., Andrade, C., Gonza´lez, J. A. and Alonso, C., (1996), A new method for in-situ measurement of electrical resistivity of reinforced concrete, *Materials and Structures*, 29, pp. 362-365.

Flick, L. D., and Lloyd, J. P., (1980), Corrosion of steel in internally sealed concrete beams under load, corrosion of reinforcing steel in concrete, ASTM STP 713, D. E. Tonini and J. M. Gaidis, eds., *ASTM International*, West Conshohocken, Pa., pp. 93-101.

Flis, J., Sehgal, A., Li D., Young, Tai K., Sabotl, S., Pickering, H., Osseo- Asare, K., Cady, P., (1993), Condition evaluation of concrete bridges relative to reinforcement corrosion: Method for measuring corrosion rate of reinforcing steel, Vol. 2. SHRP-S-324, *National Research Council*. Washington, D.C.

Francois, R., and Maso, J. C., (1988), Effect of damage in reinforced concrete on carbonation or chloride penetration, *Cement and Concrete Research*, 18, pp. 961-970.

Francois, R, Arliguie, G., (1999), Reinforced concrete: correlation between cracking and corrosion. In: Malhotra VM, editor, 2nd CANMET/ACI *International conference proceedings on durability of concrete*, vol. II. Montreal, Canada: 1999, pp. 1221–38.

Frederiksen, J. M., Nilsson, L. O., Sandberg, P., Poulsen, E., Tang, L., and Andersen, A., (1997), A system for estimation of chloride ingress into concrete, Theoretical background, *HETEK report* No. 83, The Danish Road Directorate.

Frølund, T., Klinghoffer, O. and Sørensen, H. E., (2003), Pros and cons of half-cell potentials and corrosion rate measurements, *International conference on structural faults and repairs*, London, U.K., July 1st to 3rd, 2003.

GECOR, GEOCISA, Madrid, Spain, http://www.geocisa.com.ingteyes/eindex.htm.

Gerard, B., Reinhardt, H. W. and Breysse, D., (1997), Measured transport in cracked concrete, *RILEM report 16 – Barriers to organic and contaminating liquids*, ed. Reinhardt H. W., published by E & FN SPON, London, pp. 265-324.

Gerard, B. and Marchand, J., (2000), Influence of cracking on the diffusion properties of cement-based materials, Part 1: Influence of continuous cracks on the steady-state regime, *Cement and Concrete Research*, 30(1), pp. 37-43.

Glass, G. K., (1995), An assessment of the coulostatic method applied to the corrosion of steel in concrete, *Corrosion Science*, 37(4), pp. 597-605.

Glass, G. K. and Wang Y. and Buenfeld, N.R., (1996), An investigation of experimental methods used to determine free and total chloride contents, *Cement and Concrete Research*, 26, pp. 1443-1449.

Glass, G. K. and Buenfeld, N. R., (1997), Presentation of the chloride threshold for corrosion of steel in concrete, *Corrosion Science*, 39(5), pp. 1001-1013.

Glass, G. K., Hassanein, N. M., Buenfeld, N. R., (1997), Neural network modelling of chloride binding, *Magazine of Concrete Research*, 49, pp. 323–335.

Glass, G. K., Reddy, B. and Buenfeld, N. R., (2000), The participation of bound chloride in passive film breakdown on steel in concrete, *Corrosion Science*, 42(11), pp. 2013-2021.

Goto, Y., (1971), Cracks formed in concrete around deformed tension bars, *ACI Journal Proceedings*, 68(4), Apr., pp. 244-251.

Gouda, K., (1970), Corrosion and corrosion inhibition of reinforcing steel, *British Corrosion Journal*, 5, pp. 198.

Gowers, K. R. and Millard, S. G., (1999), Measurement of concrete resistivity for assessment of corrosion severity of steel using Wenner technique, *ACI Materials Journal*, 96(5), pp. 536-542.

Haldane, D., (1976), The importance of cracking in reinforced concrete members, *Proceedings of the international conference on the performance of building structures*, Glasgow University, Plymouth, Pentoch Press, pp. 99-109, cited by Richardson, M. G., (2002), *Fundamentals of durable concrete, Modern concrete technology*, published by Spon Press, London.

Hamid, T. and Zahrani, (1990), Use of Polypropylene fibres to enhance deterioration resistance of concrete surface skin subjected to cyclic wet/dry sea waster exposure, *ACI Materials Journal*, (87), (4), pp. 363.

Hansson, C. M., Poursaee, A., and Jaffer, S. J., (2007), Corrosion of reinforcing bars in concrete, *Portland Cement Association*.

Hassanein, A., Glass, G. and Buenfled, N., (1998), The use of small electrochemcial perturbations to assess the corrosion of steel in concrete, *NDT and E International*, 31(4), pp. 265-272.

Hawkins, C. and Mckenzie, M., (1996), Environmental effects on reinforcement corrosion rates, *Proceedings of the fourth international symposium on corrosion of reinforcement in concrete construction*, pp. 166-175.

Heckroodt, R. O., 2002, *Guide to deterioration and failure of building materials*, published by Thomas Telford Ltd, 1 Heron Quay, London E14 4JD.

Hobbs, D. W., (1999), Aggregate influence on chloride ion diffusion into concrete, *Cement and Concrete Research*, 29(12), pp. 1995–1998.

Hong, K. and Hooton, R. D., (1999), Effects of cyclic chloride exposure on penetration of concrete cover, *Cement and Concrete Research*, 29, pp. 1379-1386.

Hooton, R. D. and Emery, J. J., (1990), Sulphate resistance of a Canadian slag cement, *ACI Matererials Journal*, 87(6), pp. 547–555.

Hope, B. B., Ip A. K. and Manning, D. G., (1985), Corrosion and electrical impedance in concrete, *Cement and Concrete Research*, 15(3), pp. 525 to 534.

Hunkeler, F., (2005), *Corrosion in reinforced concrete structures*, Ed. Hans B., published by Woodhead publishing limited, Abington Hall, Abington Cambridge CBI 6AH, England, pp. 1 – 45.

Ismail, M., Toumi, A., François, R. and Gagné, R., (2004), Effect of crack opening on the local diffusion of chloride in inert materials, *Cement and Concrete Research*, 34(4), April, pp. 711-716.

Jaul, W. C. and Tsay, D. S., (1998), A study of the basic engineering properties of slag cement concrete and its resistance to seawater corrosion, *Cement and Concrete Research*, 28 (10), pp. 1363–1371.

Jacobsen, S., Marchand, J. and Boisvert, L., (1998), Effect of cracking and healing on chloride transport in OPC concrete, *Cement and Concrete Research*, 26(6), pp. 869–881.

Kim, A. T. and Stewart, M. G., (2000), Structural reliability of concrete bridges including improved chloride-induced corrosion models, *Structural Safety*, 22(4), pp. 313-333

Kirkpatrick, T. J., Weyers, R. E., Anderson-Cook, C. M., and Sprinkel, M. M., (2002), Probabilistic model for the chloride-induced corrosion service life of bridge decks, *Cement and Concrete Research*, 32, pp. 1943-1960.

Kropp, J., (1995), Performance criteria for concrete durability: state of the art report, *RILEM Technical Committee 116-PCD*, published by Taylor & Francis.

Kropp, J. and Alexander, M. G., (2007), Transport mechanisms and reference tests, *chapter two, RILEM TC 189-NEC: state-of-the-art report*, Non-destructive evaluation of the penetrability and thickness of the cover, pp. 13-34.

Lambert, P., Page G. L. and Vassie P. R., (1991), Investigations of reinforcement corrosion, Electrochemical monitoring of steel in chloride-contaminated concrete, *Materials and Structures*, 24, pp. 351-358.

Leng, F., Feng, N. and Lu, X., (2000), An experimental study on the properties of resistance to diffusion of chloride ions of fly ash and blast furnace slag concrete, *Cement and Concrete Research*, 30, pp. 989-992.

Li, C. Q., Yang Y. and Melchers, R., (2008), Prediction of reinforcement corrosion in concrete and its effects on concrete cracking and strength reduction, *ACI Materials Journal*, 105(1), pp. 3-10.

Li, C. Q., (2003), Life cycle modeling of corrosion affected concrete structures-initiation, *Journal of Materials in Civil Engineering,* ASCE, 15(6).

Li, C. Q., (2001), Initiation of chloride-induced reinforcement corrosion in concrete structural members - Experimentation, *ACI Structural Journal*, 98(4), July-Aug., pp. 501-510.

LIFE-365, Service life prediction model (2005), Computer program for predicting the service life and life-cycle costs of reinforced concrete exposed to chlorides, *ACI Committee 365*.

Liu, Y., (1996), Modelling the time-to-corrosion cracking of the cover concrete in chloride contaminated reinforced concrete structures, *PhD Thesis*, Virginia Polytechnic Institute and State University.

Liu, Y. and Weyers, R. E., (1998), Modelling the time-to-corrosion cracking in chloride contaminated reinforced concrete structures, *ACI Materials Journal*, 95(6), pp. 675-681.

Luoa, R., Caib, Y. and Wang, C., Huanga, X., (2003), Study of chloride binding and diffusion in GGBS concrete, *Cement and Concrete Research*, 33 (1), pp.1-7.

Mackechnie, J. R., (1996), Predictions of reinforced concrete durability in the marine environment, *PhD Thesis*, University of Cape Town.

Machecknie, J. R., (2001), Predictions of reinforced concrete durability in the marine environment, *Research monograph No. 1*, Department of Civil Engineering, University of Cape Town.

Mackechnie, J. R., and Alexander, M. G., (2001), Repair principles for corrosion-damaged reinforced concrete structures, *Research monograph No. 5*, Department of Civil Engineering, University of Cape Town.

Mackechnie, J. R., Alexander, M. G. and Jaufeerally, H., (2003), Structural and durability properties of concrete made with Corex slag, *Research monograph No. 6*, Department of Civil Engineering, University of Cape Town.

Mackechnie, J. and Alexander, M. G., (1996), Marine exposure of concrete under selected South African conditions, *Proceedings of 3rd ACI/CANMET Int. conference on the performance of concrete in marine environment*, St. Andrews by-the-Sea, Canada, pp. 205-216.

Malhotra, V. M., (1987), Properties of fresh and hardened concrete incorporating ground granulated blast furnace slag, *Supplementary cementing materials for concrete*, ed. V. M. Malhotra, Ottawa: Canadian government publishing centre., pp. 291-331.

Mangat, P., Khatib, J. and Molloy, B., (1994), Microstructure, chloride diffusion and reinforcement corrosion in blended cement paste and concrete, *Cement and Concrete Composites*, 16, pp. 73-81.

Marcotte, T. D. and Hansson, C. M., (2007), Corrosion products that form on steel within cement paste, *Materials and Structures*, 40, pp. 325–340.

Marsavina, L., De Schutter, G., Audenaert, K., Marsavina, D. And Faur, N., (2007), The influence of cracks on chloride penetration in concrete structures. Part II – Numerical simulation, The International *RILEM Workshop on Transport Mechanisms in Cracked Concrete*, Ghent, Belgium, 3-7 September 2007.

Maslehuddin, M., (1996), Effect of temperature on pore solution chemistry and reinforcement corrosion in contaminated concrete, *The Royal Society of Chemistry*, Thomas Graham House, Science Park, Cambridge CB4 4WF, pp. 68-75.

Marta, K-K. and Jezierski, W., (2005), Evaluation of concrete resistance to chloride ion penetration by means of electrical resistivity monitoring, *Journal of Engineering Management*, 11(2), pp. 109-114.

McCarter, W. J. and Watson, D., (1997), *Proceedings of the Institute of Civil Engineers*: Structures and Buildings, 22 (2).

Mehta, P. K. and Burrows, R. W., (2001), Building durable structures in the 21st century, *Concrete International*, March, pp.57-63.

Mehta, P., (1991), Durability of concrete-Fifty years of progress, Durability of concrete, 2nd international conference, *ACI special publication -126*, Montreal, pp. 1-31.

Melchers, R. E. and Li, C. Q., (2006), Phenomenological modelling of reinforcement corrosion in marine environments, *ACI Materials Journal*, 103(1).

Metha, K. and Gerwick, B. C., (1982), Cracking–corrosion interaction in concrete exposed to marine environment, *Concrete International*.

Millard, S. G., Ghassemi, M. H, Bugey, J. Jafar M. I., (1990), Assessing the electrical resistivity of concrete structures for corrosion durability studies, corrosion of reinforcement in concrete (Eds.: Page, Treadaway, Bamforth), Elsevier, London, pp. 303-313.

Mingdong, B. and Kolluru, V. S., (2005), Corrosion of steel in cracked concrete, *Ph.D Thesis*, The City College of the City University of New York, Dept. of Civil Engineering.

Mohammed, T. U., Yamaji, T. and Hamada, H., (2003), Chloride diffusion, microstructure, and mineralogy of concrete after 15 years of exposure in tidal environment, *ACI Matererials Journal*, 99(3), pp. 256–263.

Mohamed, B., Sakai, K., Banthia, N., and Yoshida, H., (2003), Prediction of chloride ions ingress in uncracked and cracked concrete, *ACI Materials Journal*, 100(1), pp. 38-48.

Morris, W., Moreno, E. I. and Sagues, A. A., (1996), Practical evaluation of resistivity of concrete in test cylinders using a Wenner array probe, *Cement and Concrete Research*, 26(12), pp. 1779-1787

Nanukuttan, S. V., Basheer, L., McCarter, W. J., Robinson, J., and Basheer, P. A. M., (2008), Full-scale marine exposure tests on treated and untreated concretes - Initial 7-year results, *ACI Materials Journal*, 105,(1), pp. 81-87.

Nawy, E. G., Barth, F. G. and Frosch, R. J., (2001), Design and construction practices to mitigate cracking, *ACI Special Publication 204*, American Concrete Institute.

Nejadi, S., (2005), Time dependent cracking and crack control in reinforced concrete structures, *PhD Thesis*, University of New South Wales, Sydney Australia.

Neville, A. M., (1996), *Properties of concrete*, 4th Ed., Longman, New York

Neville, A. M., (1998), Concrete cover to reinforcement – or cover up?, *Concrete International*, 20(11), pp. 25-29.

Neville, A. M., (2002), Autogenous healing – A concrete miracle?, *Concrete International*, November issue, pp. 76-82.

Nilsson, A. H., and Winter G., (1985), *Design of concrete structures*, McGraw Hill.

Nilssson, L. O., Poulsen, E., Sandberg, P., Sorensen, H. E. and Klinghoffer, O., (1996), Chloride penetration into concrete, state-of-the-art, transport processes, corrosion initiation, test methods and prediction models, *HETEK Report No. 53*.

Osborne, G. J., (1999), Durability of Portland blastfurnace slag cement concrete, *Cement and Concrete Composites*, 21, pp. 11-21.

Page, C. L. and Treadaway, K. W. J., (1982), Aspects of the electrochemistry of steel in concrete, *Nature 297*, pp. 109–115.

Pal, S. C., Mukherjee, A. and Pathak, S. R., (2002), Corrosion behaviour of reinforcement in slag concrete, *ACI Materials Journal*, 99(6), pp. 1-7.

Park, R. and Pauley, T., (1975), *Reinforced concrete structures*, John Wiley and Sons, New York.

Parrott L.J. (1987), A review of carbonation in reinforced concrete, *Cement and Concrete Association*, United Kingdom, Waxham Springs, Slough.

Parrott, L., (1995), The influence of cement type and curing on the drying and air permeability of cover concrete, *Magazine of Concrete Research*, No. 171, pp. 103-111.

Paulsson, J. T. and Johan, S., (2002), Estimation of chloride ingress in uncracked and cracked concrete using measured surface concentrations, *ACI Materials Journal*, 99(1).

Pedro, M., Theodore, W. Bremner Derek, H. L., (2004), Influence of calcium nitrite inhibitor and crack width on corrosion of steel in high performance concrete subjected to a simulated marine environment, *Cement & Concrete Composites*, 26, pp. 243–253.

Perez, B. M, Zibara, H. and Hooton, R. D., (2000), A study of the effect of chloride binding on service life predictions, *Cement Concrete Research*, 30(8), pp. 1215–1223.

Pettersson, K., (1995), Chloride threshold value and the corrosion rate in reinforced concrete, *Proceedings of Nordic Seminar*, Lund.

Pettersson, K. and Jorgensen, O., (1996), The effect of cracks on reinforcement corrosion in high-performance concrete in a marine environment, *Proceedings third ACI/CANMET Int. conference on the Performance of Concrete in Marine Environment*, St. Andrews by-the Sea, Canada, pp. 185-200.

Petterson, K., and Sandberg, P., (1997), Chloride threshold levels, corrosion rates and service life for cracked high-performance concrete, *Durability of concrete, SP-170*, Vol. 1, V. M. Malhotra, ed., pp. 451-472.

Puyate, Y. T.and Lawrence, C. J., (1999), Effect of solute parameters on wick action in concrete, Chemical Engineering Science (54), pp.4257-4265.

Rasheeduzzafar, D. F. H., Al-Gahtani, A. S., Al-Saadoun, S. S. and Bader, M. A., (1990), Influence of cement composition on the corrosion of reinforcement and sulphate resistance of concrete, *ACI Materials Journal,* 87(2), pp. 114-122.

Rilem TC 154-EMC, (2000), Electrochemical techniques for measuring metallic corrosion, *Materials and Structures,* (33), pp 603-611.

Rilem TC 154-EMC, (2004), Test methods for on-site corrosion rate measurements of steel reinforced concrete by means of the polarization resistance method, *Materials and Structures*, (37), pp. 623-643.

Richardson, M. G., (2002), *Fundamentals of durable concrete, modern concrete technology*, published by Spon Press, London.

Rodriguez, P., Ramirez and Bonzalez, E J. A., (1994), Methods for studying corrosion in reinforced concrete, *Magazine of Concrete Research*, 46(167), pp. 81-90.

Rodriguez, O. G., (2001), Influence of cracks on chloride ingress into concrete, *MSc. Thesis*, University of Toronto, Graduate Department of Civil Engineering.

Rose, J., (1987), The effect of cementitious blast-furnace slag on chloride permeability of concrete, *ACI special publication SP-102: Corrosion, concrete and chlorides*, ed. F. W. Gibson, 107-25. Detroit: American Concrete Institute.

Sageus, A. A, Kranc, S. C., (1998), Computation of corrosion distribution of reinforcing steel in cracked concrete, *Proceedings of the international conference on corrosion and rehabilitation of reinforced concrete structures*, Orlando, Florida, US: University of South Florida, pp. 1–12.

Salvarezza, R., Videla, H. and Arvia, A., (1982), The electrodissolution and passivation of mild steel in alkaline sulphide solutions, *Corrosion Science*, 22(9), pp. 815-829.

Schlangen, E., Yoon, I. and De Rooij, M. R., (2007), Measurement of chloride ingress in cracked concrete, The international *RILEM workshop on transport mechanisms in cracked concrete*, Ghent, Belgium, 3-7 September 2007.

Samaha, H. R. and Hover, K. C., (1992), Influence of microcracking on the mass transport properties of concrete, *ACI Materials Journal*, 89(4), pp. 1416-1424.

Schiessl, P. ed., (1998), *Corrosion of Steel in Concrete*, Chapman and Hall Ltd: London.

Schiessl, P., and Reuter, C., (1992), Water permeability of reinforced concrete structures, state II (cracked tension zone), *No. F271*, Institute of Building Materials Research, University of Technology, Aachen.

Schiessl, P., and Edvardsen, C., (1993), Autogenous healing of cracks in concrete structures subjected to water pressure, *No. F361*, Institute of Building Materials Research, University of Technology, Aachen.

Schiessl, P. and Raupach, M., (1997), Laboratory studies and calculations on the influence of crack width on chloride-induced corrosion of steel in concrete, *ACI Materials Journal*, 94(1).

Scott, A. N., (2004), The influence of binder type and cracking on reinforcing steel corrosion in concrete, *PhD Thesis*, University of Cape town.

Sharif, A., Loughlin, K. F., Azad, A. K. and Nawaz, C. M., (1999), Determination of the effective diffusion coefficient in concrete via a gas diffusion technique, *Proceedings of the international conference on concrete durability and repair technology*, Edited by Dhir R. K. and McCarthy M. J., published by Thomas Telford.

Shi, C., (2004), Effect of mixing proportions of concrete on its electrical conductivity and the rapid chloride permeability test (ASTM C1202 or ASSHTO T277) results, *Cement and Concrete Research*, (34), pp. 537–545.

Shreir, L. ed., (1979), *Corrosion Volume 1*, Metal/Environment Reactions, Newnes-Butterworths: London cited by Scott A.N. (2004), The Influence of Binder Type and Cracking on Reinforcing Steel Corrosion in Concrete, *PhD Thesis*, University of Cape town.

Siemes, T., Schiessl, P., and Rostam, S., (2000), Future developments of service life design of concrete structures on the basis of DuraCrete, *International RILEM Workshop on Life*.

Sisomphon, K. and Franke, L., (2007), Carbonation rates of concrete containing high volume of pozzolanic materials, *Cement and Concrete Research*, 37, pp. 1647-1653.

Song, H. W. and Saraswathy, V., (2006), Studies on the corrosion resistance of reinforced steel in concrete with ground granulated blast-furnace slag—an overview, *Journal of Hazardous Materials*, 16, pp. 226-233.

Standards Australia (AS 3600), (2001), Concrete Structures, *Standards Association of Australia*, Sydney, Australia.

Stanish, K., Hooton, R. D. and Thomas, M. D. A., (2004), A novel method for describing chloride ion transport due to an electrical gradient in concrete: Part 1. Theoretical description, *Cement and Concrete Research*, 34, pp. 43–49.

Stansbury, G. and Buchanan, R., (2000), Fundamentals of Electrochemical Corrosion, ASM International, Ohio.

Stratfull, R. F., (1957), The corrosion of steel in a reinforced concrete bridge, *Corrosion*, 13, pp. 43-48.

Stern, M. and Geary, A. L. (1957), Electrochemical polarization I: theoretical analysis of shape of polarization curves, *Journal of Electrochemistry Society*, (104), pp. 56-63, cited by Poupard *et al*., (2006), Characterizing Reinforced Concrete Beams Exposed During 40 years in a Natural Marine Envirinment – Presentation of the French Project Benchmark des Poutres de la Rance, *proceedings of the 7th CANMET/ACI international conference on durability of concrete*, Montreal Canada, American Concrete Institute SP 134, pp. 17-30.

Suda, K., Misra, S. and Motohashi, K., (1993), Corrosion products of reinforcing bars embedded in concrete, *Corrosion Science*, 35(5-8), pp. 1543-1549.

Suzuki, K., Ohno, Y., Praparntanatorn, S. and Tamura, H., (1990), Mechanism of steel corrosion in cracked concrete, *Corrosion of reinforcement in concrete*, Ed. Page, C., Treadaway, K. and Bramforth, P., London: Society of Chemical Industry, pp. 19-28.

Tang, L., (1996), Chloride transport in concrete: measurement and prediction, *PhD thesis*, Publication P-96:6, Department of Building Materials, Chalmers University of Technology, Gothenburg, Sweden.

Tang, L., (2008), Engineering expression of the ClinConc model for prediction of free and total chloride ingress in submerged marine concrete, *Cement and Concrete Research*, (3).

Thomas, M. D. A., and Jones, M. R., (1996), A critical review of service life modelling of concretes exposed to chlorides, *Concrete in the service of mankind: Radical Concrete Technology*, (eds. R.K. Dhir and P.C. Hewlett), E.&F.N. Spon, London, pp. 723-736.

Torres-Acosta, A. A., and Martinez-Madrid, M., (2003), residual life of corroding reinforced concrete structures in marine environment, *Journal of Materials in Civil Engineering*, ASCE, 15(4), pp. 344-353.

Torrent, R., Alexander, M. G. and Kropp, J. (2007), Introduction and problem statement, Chapter one, *RILEM TC 189-NEC: State-of-the-art report, non-destructive evaluation of the penetrability and thickness of the cover*, pp. 1-11.

Transportation Research Circular E-C107, (2006), Control of cracking in concrete - state of the art, *Transportation Research Board*, October, Washington, DC 20001.

Trejo, D. and Pillai, R.G., (2003), Accelerated chloride threshold testing: Part I – ASTM A-615 and A-706 reinforcement, *ACI Materials Journal*, 100(6), pp. 519-527.

Tritthart, J., (1989), Chloride binding in cement – I: Investigations to determine the composition of pore water in hardened cement, *Cement and Concrete Research*, 19, pp. 586-594.

Tritthart, J., (1989), Chloride binding: II, The influence of the hydroxide concentration in the pore solution of hardened cement paste on chloride binding, *Cement and Concrete Research*, (19), pp. 683–691.

Tromans, D., (1980), Anodic polarization behaviour of mild steel in hot alkaline sulfide solutions, *Journal of Electrochemical Society*, June, pp. 1253-1256 cited by Scott A.N. (2004), The influence of binder type and cracking on reinforcing steel corrosion in concrete, *PhD Thesis*, University of Cape town.

Tuutti, K., (1982), Corrosion of steel in concrete, *Swedish Cement and Concrete Research Institute*, Stockholm, Report No.CBI Research 4:82, pp. 468.

Tuutti, K., (1993), Effect of cement type and different additions on service life. In: R.K. Dhir and M.R. Jones, Editors, *Proceedings of the international conference concrete 2000 – economic and durable construction through excellence*, E&FN Spon, London, pp. 1285–1295.

Uhlig, H. H., (1971), *Corrosion and Control*, published by John Wiley and Sons Inc., New York.

Valentini, C., Berardo, L. and Alanis, I., (1990), Influence of blast furnace slags on the corrosion rate of steel in concrete, Corrosion rates of steel in concrete, *ASTM STP 1065*, Philadelphia, pp. 17-28.

Vienna, (2002), Guidebook on non-destructive testing of concrete structures, *International Atomic Energy Agency*.

Wang, K., Daniel, C. J. and Surendra, P. S., (1997), Permeability study of cracked concrete, *Cement and Concrete Research*, 27(3), pp. 381-393.

Wang, X. M. and Zhao, H. Y., (1993), The residual service life prediction of R.C. structures, cited by S. Nagataki *et al*., *Durability of building materials and components*, E & FN Spon, pp. 1107–1114.

Weiss, J., Radalinska, A., Paradis, F., Niemuth, M. and Sant, G., (2007), Cracks in concrete: An overview of an approach to assess their development, their physical features, and their impact on durability, The international *RILEM workshop on transport mechanisms in cracked concrete*, Ghent, Belgium, 3-7 September 2007.

West, J., (1980), *Basic Corrosion and Oxidation*, Ellis Horwood Limited, London.

Whiting, D. A. and Nagi, M. A., (2003), Electrical resistivity of concrete—A literature review, *Portland Cement Association*, Illinois, pp 56.

Wood, S. L., (1981), Twenty years of experience with slag cement, *Symposium on slag cement*, University of Alabama, Birmingham, April 30 – May 1, 1981.

Yong, Ki Ann and Song Ha-Won, (2007), Chloride threshold level for corrosion of steel in concrete, *Corrosion Science*, 49(11), pp. 4113-4133.

Yoon, S., Wang, K., Weis, W. J., and Shah, S. P., (2000), Interaction between loading, corrosion, and serviceability of reinforced concrete, *ACI Materials Journal*, 97(6), pp. 637-644.

Zivica, (2003), Influence of w/c ratio on rate of chloride induced corrosion of steel reinforcement and its dependence on ambient temperature, *Bull. Materials Science*, 26(5), pp. 471–475.